Understanding vapor nucleation on the molecular level: A review

Understanding Vapor Nucleation on the Molecular Level: A Review

Chenxi Li[1*] and Ruth Signorell[2]

[1]School of Environmental Science and Engineering, Shanghai Jiao Tong University, Shanghai 200240, China;

[2]Department of Chemistry and Applied Biosciences, ETH Zürich, Vladimir-Prelog-Weg 2, CH-8093 Zürich, Switzerland.

*Corresponding author: chenxi20@sjtu.edu.cn

Abstract:

Gas phase nucleation is a universal phenomenon that plays a crucial role in both natural settings and industrial processes. Despite more than 100 years' work to decipher this highly dynamic process, our understanding of nucleation remains incomplete. In particular, the formation, decay, and structures of the initially formed nucleating clusters critically determine the overall behavior of the nucleation systems, yet they are elusive to conventional experimental methods that only detect grown particles. Filling this gap of understanding calls for the ability to probe nucleation on a molecule-by-molecule basis to retrieve direct evidence of nucleation pathways and the temporal evolution of the nucleating clusters. In this review, we summarize recent modelling and experimental efforts to meet this demand. The techniques discussed here have offered unprecedented molecular level insight into the nucleation process, but they are still subject to constraints in terms of applicable scope and measurement uncertainties. We shall highlight both the advantages and limitations of each technique, with the hope that this review can lead to novel applications and further improvements of the introduced methods.

Keywords:

nucleation, new particle formation, molecular-level, clusters, nucleation modelling, nucleation experiment

1. Introduction

The formation of new condensed phase particles from gas phase precursors is a crucial element in the atmosphere and in a variety of industrial processes. In the atmosphere, new particle formation influences the concentration of cloud condensation nuclei (Dunne et al., 2016; Kuang, McMurry, & McCormick, 2009; Merikanto, Spracklen, Mann, Pickering, & Carslaw, 2009; Riipinen et al., 2011; Spracklen et al., 2008; Westervelt, Pierce, & Adams, 2014), and relates to hazing episodes with severe adverse health effects (Guo et al., 2020; Guo et al., 2014). In industry, particle formation is sometimes intentionally induced, e.g. to synthesize nanoparticles (Kammler, Mädler, & Pratsinis, 2001; Li, Ren, Biswas, & Tse, 2016) or to separate gas mixtures (Haghighi, Hawboldt, & Abedinzadegan Abdi, 2015), but in other circumstances should be carefully regulated as in steam turbines (Ahmad, Casey, & Sürken, 2009) and high speed wind tunnels (Daum, 1963). The initial step of particle formation, referred to as nucleation, is the process where molecules interact to form thermodynamically stable molecular clusters. An in-depth understanding of nucleation is critical to quantify nucleation rates in planetary atmospheres and to optimize industrial processes.

Since C. J. Wilson's pioneering expansion cloud chamber experiments (Wilson, 1897), considerable theoretical, modelling and experimental efforts have been devoted to unveiling the detailed mechanisms of nucleation in various systems of interest. Ideally, if we can track the temporal evolution of cluster size distributions in a nucleation event, with the cluster size and composition resolved on the molecular level, all the information required to elucidate nucleation mechanisms can be extracted. However, until recently only the distributions of grown particles, i.e. particles larger in size than the smallest, thermodynamically stable molecular clusters (the critical nucleus), were routinely quantified (with uncertainties, see Kangasluoma and Kontkanen (2017) and Kangasluoma et al. (2020)). Several experimental challenges, the relative importance of which depends on the context, hinder our effort to study nucleation on a molecular basis.

The first and foremost challenge comes from the difficulty in the detection of nucleating clusters. In any nucleation event, the propensity of nucleating clusters to grow and decay essentially determines the nucleation pathways and the nucleation rate. However, nucleating clusters are often low in concentrations and fragile , hence their detection is ultra-demanding on instrument sensitivity and the instrument's ability to preserve cluster integrity. For instance, the most frequently applied technique to detect nucleating clusters, i.e. mass spectrometry, requires the neutral nucleating clusters to be ionized for detection. Even with the relatively soft chemical ionization method, the clusters could go through severe transformations upon ionization and during transmission (Brophy & Farmer, 2016; Ortega et al., 2016; Passananti et al., 2019; Zapadinsky, Passananti, Myllys, Kurtén, & Vehkamäki, 2019), not to mention if more conventional

ionization methods, e.g. electron ionization, are applied (Fárník & Lengyel, 2018). In fact, recent progress on nucleation characterization critically relies on detection methods that minimize cluster fragmentation to a better extent (Eisele & Hanson, 2000; Eisele & Tanner, 1993; Litman, Yoder, Schläppi, & Signorell, 2013; Schläppi, Litman, Ferreiro, Stapfer, & Signorell, 2015).

The second challenge originates from the complex chemical environments in which nucleation takes place. This is particularly the case for atmospheric nucleation events, where potential nucleation participants are numerous (Kerminen et al., 2018; Kulmala et al., 2014; Lee et al., 2019). It is often difficult to pinpoint which chemical species participates in nucleation since not every nucleating species can be detected by instruments or quantified with a sufficient level of accuracy. A notable example of 'undetectable species' in nucleating cluster measurements is water. Although humidity is known to influence nucleation rates (Chen et al., 2015; Dunne et al., 2016; Henschel, Kurtén, & Vehkamäki, 2016; Henschel et al., 2014; Kildgaard, Mikkelsen, Bilde, & Elm, 2018a, 2018b; Yu et al., 2017), water is mostly missing from the mass spectra measured during atmosphere nucleation events. One must resort to indirect measurements and modelling to infer the cluster hydration states.

The third experimental challenge arises from the transient nature of nucleation. This is less of a problem for atmospheric nucleation events that can last up to hours, but poses an obstacle for laboratory nucleation studies that employ highly supersaturated vapors with high nucleation rates. In these studies, nucleation typically runs its course on a millisecond- or microsecond- time scale (Wyslouzil & Wölk, 2016), shorter than the time-resolution of the measuring device. As a result, the measurable quantity from these experiments is the number concentration (in fewer cases, size distributions) of grown particles that does not directly unveil molecular level details of the nucleation process. To extract molecular level information from these studies, the measuring device must be designed to take several snapshots of the cluster size distribution within the time-window of nucleation (Schläppi et al., 2015).

Efforts to improve nucleation instrumentation mainly focus on overcoming the aforementioned challenges. Though a lot of important nucleation scenarios remain unexplored, nowadays nucleation can indeed be observed on the molecular level. Apart from improvement of measurement techniques, the advancement of modelling techniques, e.g. quantum mechanical calculations and molecular dynamic simulations, has greatly facilitated our understanding of the nucleation process. In this review, we set out to summarize and comment on the existing tools that provide molecular-level information on the nucleation process, with the content organized as follows: We begin by introducing basic concepts and theoretical frameworks to understand nucleation in sections 2.1-2.3. We then review modelling techniques including GDE-based kinetic simulations, molecular cluster structure and energy calculations, and molecular dynamics simulations in sections 2.4-2.6, respectively. In section 3, we turn to experimental techniques that

characterize nucleation on the molecular level. Specifically, we focus on nucleation measurements in the postnozzle flow of Laval expansions and the characterization of atmospheric nucleating clusters. We limit ourselves to the 'molecular level' understanding of the nucleation process, hence important techniques that can identify the chemical compositions and size distributions of grown particles are not included here. These important topics are discussed in recent complementary reviews (Johnston & Kerecman, 2019; Kangasluoma et al., 2020). Furthermore, in this review we do not discuss heterogeneous nucleation, i.e. nucleation of vapors on pre-existing nuclei (Gamero-Castaño & de la Mora, 2002; Tauber et al., 2018; Winkler et al., 2008; Winkler et al., 2012). The theoretical aspect of heterogeneous is different from the homogenous nucleation theory presented in section 2.2-2.3, and we refer the reader to the cited works (Fletcher, 1958; Gamero-Castaño & de la Mora, 2002; Vehkamäki et al., 2007) for more details.

2. Nucleation theories and modelling techniques

In this section we briefly review gas phase nucleation theories and modelling techniques. Basics of the nucleation thermodynamics and kinetics are introduced in section 2.1, followed by a discussion of the key points in the classical nucleation theory (section 2.2) and the nucleation theorems (section 2.3). Detailed, in-depth accounts of nucleation theories are found in textbooks written by Kashchiev (2000), Vehkamäki (2006), and Kalikmanov (2013). Following the theoretical discussions, we look into three molecular-level modelling techniques applied in nucleation research, i.e. GDE-based kinetic modelling, cluster structure and energy simulations, and molecular dynamic simulations.

2.1 Nucleation thermodynamics and kinetics

Gas phase nucleation can be viewed as the overcoming of an energy barrier by vapor molecules to form clusters that spontaneously grow. As most nucleation experiments take place at (near-) constant pressure and temperature, the Gibbs free energy is the chosen quantity for the cluster free energy of formation. For a system with a single nucleating vapor (unary nucleation), the Gibbs free energy of formation (Oxtoby & Kashchiev, 1994) of a *k*-mer (a molecular cluster containing *k* molecules) is given by

$$\Delta G_k = k\Delta\mu + F(k) \tag{1}$$

where $\Delta\mu$ is the chemical potential difference between the condensed and vapor phase, $F(k)$ is the cluster surface energy. A simplified version of ΔG_k variation as a function of k is shown in Fig. 1. If the vapor saturation ratio S is less than 1, both $k\Delta\mu$ and $F(k)$ are positive and increases with cluster size. Nucleation is forbidden by this ever-increasing energy barrier. As S rises above 1, $k\Delta\mu$ becomes negative but nucleation is still hindered by the creation of cluster surface ($F(k) > 0$). This leads to ΔG_k to first increase and then decrease with k, shown by the blue solid line in Fig. 1. Gas-to-particle transition occurs but at a

suppressed rate because the formation of the smallest clusters is thermodynamically unfavorable. Nucleation rates thus represent the frequency at which thermal fluctuations drive the clusters past the energy barrier. The term 'nucleation' was coined to refer to phase transition in such a scenario. As S further increases, the decrease in chemical potential defeats the increase of the surface term for all clusters (ΔG_k<0 for $k \geq 2$). Cluster formation thus proceeds without an energy barrier (barrierless nucleation). Barrierless nucleation has been observed in atmospheric nucleation studies (Kürten et al., 2014; Kürten et al., 2018) and in low-temperature nucleation systems (Chakrabarty, Ferreiro, Lippe, & Signorell, 2017; Krohn, Lippe, Li, & Signorell, 2020). In many atmospheric nucleation events, it is unclear if nucleation proceeds with or without a barrier. Therefore, in atmospheric studies the term 'new particle formation (NPF)' is often used to describe the gas-to-particle phase transition. In this review, we use 'nucleation' as a generic term to describe the gas-to-particle transition because the tools we later introduce apply to nucleation with and without a barrier.

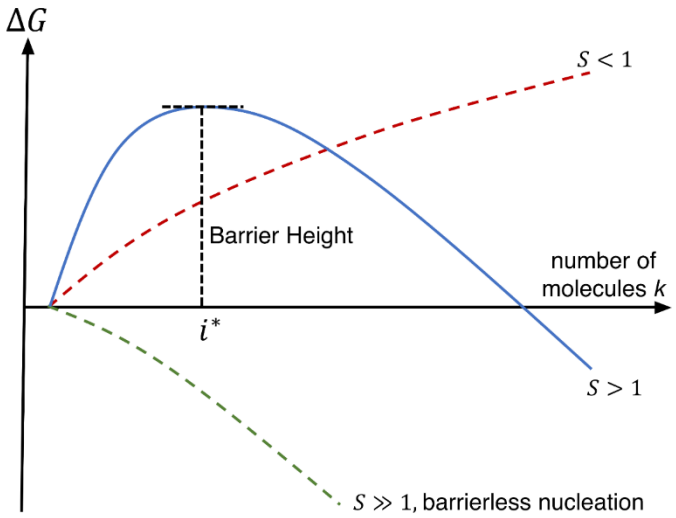

Fig. 1. The Gibbs free energy of cluster formation as a function of cluster size.

Eq. (1) describes the nucleating clusters from a thermodynamic perspective, but nucleation is fundamentally a kinetic process: monomers/clusters constantly collide with each other to form bigger clusters, while at the same time clusters go through dissociation to replenish monomers/smaller clusters. For a spatially homogeneous, unary nucleation system, the time evolution of the number concentration (N_k) of k-mers is governed by the following equation,

$$\frac{\mathrm{d}N_k}{\mathrm{d}t} = \frac{1}{2}\sum_{i+j=k}\beta_{i,j}N_iN_j - N_k\sum_{j=1}^{\infty}\beta_{k,j}N_j - E_kN_k + E_{k+1}N_{k+1} - L_k + S_k(k \geq 2) \qquad (2)$$

where $\beta_{i,j}$ is the association rate constant of cluster *i* and cluster *j*, E_k is the evaporation rate of the *k*-mers , L_k and S_k represent loss and production rates of *k*-mers by mechanisms other than coagulation, condensation and evaporation. Eq. (2) and its equivalent variations are referred to as the general dynamic equations (GDE, (Gelbard & Seinfeld, 1979)), the birth-death equations (Vehkamäki & Riipinen, 2012) or population balance equations. Implicit in Eq. (2) are the assumptions that clusters do not fragment upon collisions with monomers or clusters, and that only molecules evaporate from clusters. If spatial inhomogeneity exists, additional terms need to be introduced to account for spatial transport (Cai et al., 2018; Kommu, Khomami, & Biswas, 2004a, 2004b). Provided monomers are much higher in concentration compared to molecular clusters, the cluster-cluster association (coagulation) terms in Eq. (2) can be ignored. With the additional constraint that both L_k and S_k are negligible, Eq. (2) reduces to the Becker-Döring equation (Becker & Döring, 1935),

$$\frac{\mathrm{d}N_k}{\mathrm{d}t} = \beta_{1,k-1}N_1N_{k-1} - \beta_{1,k}N_1N_k - E_kN_k + E_{k+1}N_{k+1}\ (k \geq 2). \tag{3}$$

The nucleation thermodynamics (Eq. (1)) and kinetics (Eqs. (2) and (3)) are related by detailed balance at equilibrium conditions. For an isothermal nucleation system, $\beta_{1,k}$, E_{k+1} and ΔG are interrelated by the following equation,

$$E_{k+1} = \beta_{1,k}N_1 \exp\left(\frac{\Delta G_{k+1}(T,N_1) - \Delta G_k(T,N_1)}{k_\mathrm{B}T}\right). \tag{4}$$

where k_B is the Boltzmann constant, T is the temperature and $\Delta G_k(T, N_1)$ is the Gibbs free energy of formation of *k*-mers from monomers at the monomer concentration N_1. In the next section we show how the classical nucleation theory is formulated based on Eqs. (1), (3) and (4).

2.2 The classical nucleation theory

The classical nucleation theory (CNT) is an easy-to-implement theory that only requires bulk material properties as inputs. With the advances in both nucleation theories and modelling techniques, nowadays CNT is less often applied with the purpose to predict nucleation rates, but more often used as a reference for other nucleation theories and experimental studies. Nonetheless, the framework of CNT is fundamentally sound within assumptions and can be quite powerful when combined with more accurate cluster energetics (see section 2.5). Here we give a brief outline of CNT to serve as a basis for further discussion.

The formulation of CNT for a single-component (unary) system starts by assuming nucleation reaches *steady state*, i.e., $\frac{\mathrm{d}N_k}{\mathrm{d}t}$ in Eq. (3) is zero. Eq. (3) can then be analytically solved (Seinfeld & Pandis, 2016) to give the following expression for the nucleation rate *J*,

$$J = N_1 \left(\sum_{i=1}^{\infty} \frac{1}{N_1 \beta_{1,i} \prod_{j=1}^{i-1} \frac{N_1 \beta_{1,j}}{E_{j+1}}} \right)^{-1} . \quad (5)$$

In Eq. (5), J is expressed as a function of a series of rate coefficients, among which the evaporation rates are largely unknown. As Eq. (4) relates the Gibbs free energy to the kinetic coefficients, we substitute Eq. (4) into Eq. (5), leading to

$$J = \frac{N_1^2}{\sum_{i=1}^{\infty} \frac{\exp\left(\frac{\Delta G_i(T,N_1)}{k_B T}\right)}{\beta_{1,i}}} . \quad (6)$$

Eq. (6) gives a simple formula to calculate the nucleation rate, but requires ΔG_i's as inputs. In CNT, ΔG_i is approximated by the capillary approximation, i.e.

$$\Delta G_i = -(i-1) k_b T \ln S + \sigma(A_i - A_1), \quad (7)$$

where σ is the surface tension of the bulk material at temperature T, A_i is the surface area of the cluster i assuming the clusters are well-defined spheres with a uniform density. Since the denominator of Eq. (6) depends exponentially on ΔG_i's, it can be approximated by integration around the maximum of ΔG_i, leading to the simplified form of the nucleation rate,

$$J_{\mathrm{CNT}} = K \exp\left(-\frac{\Delta G^*}{k_B T}\right), \quad (8)$$

where K is a kinetic prefactor and ΔG^* is the formation free energy of the critical nucleus. The size of the critical nucleus at which ΔG_i reaches the maximum is given by

$$i^* = \frac{32\pi\sigma^3 v^2}{3(k_B T)^3 (\ln S)^3}, \quad (9)$$

where v is the volume of the monomer. For binary nucleation, the derivation of CNT is more involved, but the final form of the nucleation rate is similar,

$$J_{bin} = K_{bin} \exp\left(-\frac{\Delta G^*_{bin}}{k_B T}\right), \quad (10)$$

$$\Delta G_{bin} = n_1 \Delta\mu_1 + n_2 \Delta\mu_2 + \sigma_{bin} A_{bin}, \quad (11)$$

where the subscript 'bin' indicates 'binary', n_i is the number of molecules of component i in the cluster, $\Delta\mu_i$ is the change of chemical potential from the vapor phase to the condensation phase. ΔG^*_{bin} is located on a saddle point in the two-dimensional free energy surface.

From the derivation above, some limitations of CNT are easily identifiable. First, CNT calculates the steady-state nucleation rates without providing any information on the process leading to the steady state. Second, CNT only applies to isothermal nucleation, i.e. the nucleating clusters are at the same temperature as the surrounding. This limitation is explicitly manifested by Eq. (7) in which T is set to the ambient temperature. In experiments/simulations where the carrier gas is not present in sufficiently high concentrations to fully thermalize the nucleating clusters to the ambient temperature (Halonen, Zapadinsky, & Vehkamäki, 2018; Wyslouzil & Seinfeld, 1992), non-isothermal corrections (Feder, Russell, Lothe, & Pound, 1966) must be applied to the nucleation rate. Lastly but most importantly, the capillary approximation leads to large errors of cluster formation energies, in particular for small clusters with highly curved surfaces. Embedded in the capillary approximation is also the wrong interpretation that the nucleating clusters have a uniform density with a well-defined spherical shape, while in reality cluster density should transition gradually from the core to the gas phase (Angélil, Diemand, Tanaka, & Tanaka, 2014) and clusters might be fractal rather than spherical (Kathmann, Schenter, Garrett, Chen, & Siepmann, 2009). These drawbacks of CNT can be partially mitigated by resorting to more advanced computational methods, e.g. quantum chemical calculations, to obtain cluster formation energies (section 2.5).

2.3 The nucleation theorems

A powerful, yet often misused tool to retrieve the critical cluster size is the first nucleation theorem. This theorem was first proposed by Kashchiev (1982) for unary, gas phase nucleation systems, with the aim to retrieve critical cluster sizes independent of the underlying nucleation theories; it was later extended to multicomponent nucleation by Oxtoby and Kashchiev (1994). The derivation proposed by Kashchiev is based on thermodynamics, but the first nucleation theorem can also be formulated by a kinetic approach based on the law of mass action (Bowles et al., 2000; McGraw & Wu, 2003). For a unary system, the first nucleation theorem reads

$$i_T^* \cong \left(\frac{d\ln J}{d\ln S}\right)_T - \left(\frac{d\ln K}{d\ln S}\right)_T , \tag{12}$$

where i_T^* is the number of molecules in the critical nucleus. For binary systems, the first nucleation theorem is given by

$$i_1^* \cong \left(\frac{d\ln J_{bin}}{d\ln a_1}\right)_{a_2,T} - \left(\frac{d\ln K_{bin}}{d\ln a_1}\right)_{a_2,T} \tag{13}$$

and

$$i_2^* \cong \left(\frac{d\ln J_{bin}}{d\ln a_2}\right)_{a_1,T} - \left(\frac{d\ln K_{bin}}{d\ln a_2}\right)_{a_1,T}, \tag{14}$$

where i_j^* is the number of molecules in the critical nucleus of component j, a_j is the gas phase activity of component j. The first nucleation theorem has been applied to analyze data from numerous measurements (Brus, Hyvärinen, Ždímal, & Lihavainen, 2005; Kuang, McMurry, McCormick, & Eisele, 2008; Looijmans, Luijten, & van Dongen, 1995; Manka et al., 2010; McGraw & Zhang, 2008; Viisanen & Strey, 1994; Zollner et al., 2012) and molecular dynamics simulations (Matsubara, Koishi, Ebisuzaki, & Yasuoka, 2007; Napari, Julin, & Vehkamäki, 2009). From Eqs. (12-14), the implementation of the nucleation theorem requires a set of nucleation rate measurements at varying saturation levels at a fixed temperature and activities of other components. This requirement might be loosened if the logarithm of the nucleation rate is linear with respect to the logarithm of component concentrations over a wide nucleation rate range (McGraw & Zhang, 2008).

Despite being a convenient tool to derive critical cluster sizes, the first nucleation theorem has rather restrictive underlying assumptions. These assumptions have been summarized and tested against simulations by Kupiainen-Määttä et al. (2014) (see Table 1 in the cited work; other works that discuss the restrictions of the nucleation theorem include Ehrhart and Curtius (2013), Vehkamäki et al. (2012) and Malila, McGraw, Laaksonen, and Lehtinen (2015)). Some of these restrictions include the single high nucleation energy barrier, negligible coagulation, and the absence of external particle losses. In general, the first nucleation theorem cannot be naively applied without all inherent assumptions satisfied. For instance, the scavenging of nucleating clusters by pre-existing particles can affect the power dependence of the nucleation rate on the concentration of the nucleating species, leading to wrong interpretation of the critical cluster size if Eqs. (12-14) are applied (see Fig. 3 and Fig. 4 in Kupiainen-Määttä et al. (2014)). Therefore, literature-reported critical cluster sizes determined from the nucleation theorem should be treated critically, especially in atmospherically relevant studies in which particle sinks (particle wall losses, scavenging by pre-existing particles) strongly affect the nucleation process.

The second nucleation theorem (Ford, 1996, 1997; Vehkamäki & Ford, 2000) gives the excess internal energy of the critical cluster, $E_x(n^*)$, which is the energy difference between molecules in the cluster and molecules in the bulk condensed phase. For a unary system, the second nucleation theorem reads

$$E_x(n^*) \cong k_{\mathrm{B}}T^2\left(\frac{d\ln J}{d\mathrm{T}}\right)_{\ln S} + k_{\mathrm{B}}T - L, \tag{15}$$

where L is the latent heat of condensation per molecule. $E_x(n^*)$ retrieved with the second nucleation theorem can be compared with theoretical predictions to better understand the nucleation mechanisms. Tanimura, Pathak, and Wyslouzil (2013) compared the excess energy of pure water clusters from the second nucleation theorem and that from quantum chemical calculations. This comparison suggests a constant

nucleation prefactor independent of monomer concentration, which might be caused by insufficient cooling of the critical nucleus at highly saturated conditions. Ogunronbi and Wyslouzil (2019) calculated $E_x(n^*)$ for the critical clusters during pentane, hexane and heptane nucleation and found an overall stronger dependence of $E_x(n^*)$ on $n*$ than predicted by the capillary approximation.

2.4 GDE-based kinetic simulations

Solving the general dynamic equations (GDE, Eqs. (2) and (3)) produces the cluster size distributions as a function of time (Ehrhart et al., 2016; Lovejoy, Curtius, & Froyd, 2004; McGrath et al., 2012; McMurry & Li, 2017; Wyslouzil & Wilemski, 1995; Yu, 2006; Yu et al., 2018). Added to that, using numerical approximation methods, e.g. the discrete-sectional method or the collocation method (Gelbard & Seinfeld, 1978; Gelbard, Tambour, & Seinfeld, 1980; Wu & Flagan, 1988), particle size distributions up to tens of micrometers can be computed at a small computational cost. This coverage of the whole particle size range makes GDE-based simulations a powerful tool, allowing the testing of the proposed nucleation mechanisms/theories against the experimentally observable particle size distributions (Kürten et al., 2018). To date, GDE-based kinetic analysis have been applied to predict nucleation rates (Yu, 2006; Yu et al., 2018), extract rate constants (Jen, McMurry, & Hanson, 2014; Li, Lippe, Krohn, & Signorell, 2019), identify nucleation mechanisms (Kürten et al., 2018), and examine the significance of physical/chemical processes (Kupiainen-Määttä et al., 2014; Li & McMurry, 2018; Liu et al., 2019; McMurry & Li, 2017). The kinetic equations can be further coupled with gas phase reaction schemes to incorporate gas phase chemistry (Carlsson et al., 2020; Carlsson & Zeuch, 2018), or combined with fluid dynamics equations to capture spatial characteristics of particle nucleation and growth (Kommu et al., 2004a, 2004b).

Despite being a straightforward approach, a few challenges stand in the way of wider applications of the GDE-based kinetic simulations. Elm et al. (2020) put up a checklist that researchers should consult while implementing GDE-based kinetic simulations (the terminology used in their work is 'cluster dynamics simulations'). Here we selectively comment on two challenges complementary to their work. First, we note that a full kinetic modelling of multi-component nucleation systems inclusive of all possible cluster compositions is exceedingly complex. To mitigate the complexity one can either truncate some of the nucleation pathways (Jen et al., 2014), or to adopt simplification methods to replace kinetics with equilibrium distributions (Carlsson et al., 2020; Yu et al., 2018). For instance, in systems that contain a less volatile nucleating species X and a more volatile species Y, a cluster experiences many collisions with Y-molecules in between collisions with X-molecules. This allows modelling the distribution of clusters X_iY_j as in thermal equilibrium with species Y. Yu et al. (2018) adopted this strategy in their modelling of the multicomponent system including sulfuric acid, water, ammonia and ions: the clusters are assumed to be in equilibrium with both gas phase ammonia and water.

Second, the solution of the GDE equations requires rate constants as inputs, i.e. the evaporation rate of a j-mer (E_j) and association rate between an i-mer and a j-mer ($\beta_{i,j}$) must be fed into a numerical GDE solver. In practice, E_j is computed with Eq. (4) for a fully thermalized cluster at temperature T, while $\beta_{i,j}$ can be approximated by the hard-sphere collision rate frequency function ($\beta_{i,j,hs}$). Apparently, the computation of E_j requires ΔG_j, which used to be approximated with the liquid droplet model as in CNT (Rao & McMurry, 1989), but is increasingly obtained from the quantum chemical calculations (see section 2.5). Because of the exponential dependence, E_j is highly sensitive to the accuracy of ΔG_j. This introduces large uncertainties to the kinetic modelling even if ΔG_j is based on quantum chemistry (with the best achievable accuracy around ± 1 kcal/mol). In contrast, using $\beta_{i,j,hs}$ as a substitue for $\beta_{i,j}$ usually leads to smaller errors, but $\beta_{i,j}$ can still deviate from $\beta_{i,j,hs}$ in both directions. First, in the calculation of $\beta_{i,j,hs}$, the cluster shape is often assumed to be spherical with its density taken to be the bulk density – this can be a very rough approximation for the molecular clusters (Angélil et al., 2014). Second, long range interactions, e.g. Van der Waals forces, dipole-dipole interactions, dipole-ion interactions, can lead to enhanced $\beta_{i,j}$. This enhancement has been known in the aerosol community for particle coagulations (Ouyang, Gopalakrishnan, & Hogan, 2012; Sceats, 1989) and has been investigated on the molecular level using molecular dynamics simulations (Halonen, Zapadinsky, Kurtén, Vehkamäki, & Reischl, 2019; Yang, Goudeli, & Hogan, 2018) and through experiments (Krohn et al., 2020; Li et al., 2019; Stolzenburg et al., 2020). Third, $\beta_{i,j}$ can be smaller than the hard sphere rate as 'collisions' does not necessarily lead to formation of newly coalesced clusters, i.e. the accomodation coefficient is less than unity. This may originate from steric effects specific to the molecular and cluster structures, or from energy nonaccomodation, i.e. the excess translational energy released in cluster formation (Yang, Drossinos, & Hogan, 2019) leads to instant breakup of the newly formed, metastable clusters (Kurtén et al., 2010). At atmospheric conditions, energy non-accomodation is less of a concern because the high-concentration air molecules instantly take away the excess energy to stabilize the clusters. Hydration of the colliding entities, common at atmospheric conditions, also facilitates the allocation of the excess energy (Kurtén et al., 2010; Loukonen, Bork, & Vehkamäki, 2014a). However, at low pressures, $\beta_{i,j}$ can deviate from $\beta_{i,j,hs}$ by orders of magnitude. For instance, the association rate of two water monomers have been found to be considerably lower than the monomer-monomer collision rates from both theories and experiments (Bourgalais et al., 2016; Lippe, Chakrabarty, Ferreiro, Tanaka, & Signorell, 2018). It is currently unclear to what extent the deviation of $\beta_{i,j}$ from collision rates can affect nucleation estimation under various experimental conditions, but one could expect energy non-accommodation to play a more important role at reduced pressures.

2.5 Cluster structure and free energy calculations

GDE-based kinetic simulations are useful for generating cluster size distributions but shed no light on cluster structures and formation energies. Three molecular-level computational methods, i.e. quantum chemistry (QC) calculations, Monte-Carlo (MC) simulations and molecular dynamics (MD) simulations, help fill this gap. Among these methods, QC calculation is based on first principles of quantum mechanics with the highest level of accuracy in terms of cluster energy (uncertainties down to $\pm$ 1 kcal/mol). However, accurate QC calculations are limited to relatively small clusters because of computational cost. In contrast, both MC and MD simulations (Frenkel & Smit, 2002) are mostly based on atomic force fields and are applicable to larger clusters with decreased accuracy. Since the experimental detection and analysis of molecular clusters is still exceedingly challenging, these simulations offer insight on nucleating cluster properties that are otherwise unavailable.

The application of QC to simulate nucleating clusters has seen rapid increase in recent years, especially in atmospheric-relevant nucleation studies. State-of-the-art QC methods applied to atmospheric nucleating clusters are comprehensively reviewed by Elm et al. (2020). Here we only briefly summarize the main applications of QC simulations:

1. QC-based cluster Gibbs free energies can be substituted into the CNT framework, e.g. Eq. (5), to calculate nucleation rates. Nucleation rates calculation with QC-based free energies often show improved performance compared to CNT predictions (Bromley, Gómez Martín, & Plane, 2016; Du, Nadykto, & Yu, 2009; Duplissy et al., 2016; Goumans & Bromley, 2012; Krohn et al., 2020; Merikanto et al., 2016).
2. Through Eq. (4), QC-based cluster free energy can be used to infer cluster evaporation rates, which are inputs to GDE-based kinetic models introduced in the previous section (Carlsson et al., 2020; McGrath et al., 2012). These evaporation rates also provide a benchmark against which experimentally extracted rates can be compared (Jen et al., 2014; Ortega et al., 2012).
3. QC calculations play an essential role in estimating the extent of hydration for the atmospheric nucleating clusters (Henschel et al., 2016; Henschel et al., 2014; Kildgaard et al., 2018a, 2018b; Kurtén, Noppel, Vehkamäki, Salonen, & Kulmala, 2007; Loukonen et al., 2010; Rasmussen et al., 2020; Temelso et al., 2012) since water molecules evaporate almost completely even in the state-of-the-art atmospheric cluster detection methods.
4. QC calculations help identify the key nucleating species and potential nucleation pathways by examining the cluster stability (Bork, Elm, Olenius, & Vehkamäki, 2014; Elm, Jen, Kurtén, & Vehkamäki, 2016; Elm, Kurtén, Bilde, & Mikkelsen, 2014; Elm, Passananti, Kurtén, & Vehkamäki, 2017; Lin et al., 2019; Myllys, Elm, Halonen, Kurtén, & Vehkamäki, 2016; Ortega et al., 2016;

Ortega et al., 2012; Xu & Zhang, 2012; Zhao, Khalizov, Zhang, & McGraw, 2009). For instance, through QC simulations Elm, Myllys, and Kurtén (2017) proposed that that an organic oxidation product can stabilize sulfuric acid clusters if the molecule has no or weak intramolecular hydrogen bonds and at least two carboxylic acid groups. Another example is the computational study by Liu et al. (2019) , in which methanol is found to have a quenching effect on NPF by scavenging SO_3 to form methyl hydrogen sulfate.

QC calculations are performed on many different levels, leading to difficulties of data inter-comparison from different works. Recently, 633 unique atmospherically relevant molecular clusters were compiled into a database with the cluster structure and vibrational frequency calculated on the ωB97X-D/6-31++G(d,p) level of theory and single point cluster energy calculated with DLPNO-CCSD(T)/aug-cc-pVTZ (Elm, 2019). Such a database is one step towards constructing comprehensive kinetic models to simulate atmospheric new particle formation.

Compared to QC, MC simulations have seen more applications in fundamental nucleation studies. Nucleating clusters examined by MC mainly include Lenard-Jones clusters (ten Wolde & Frenkel, 1998), water clusters (Merikanto, Vehkamäki, & Zapadinsky, 2004; Merikanto, Zapadinsky, Lauri, & Vehkamäki, 2007) and clusters formed in binary/multicomponent systems (Chen, Siepmann, & Klein, 2003; Chen, Siepmann, Oh, & Klein, 2001; McKenzie & Chen, 2006; Nellas & Chen, 2008; Nellas, Keasler, Siepmann, & Chen, 2010; Ogunronbi, Sepehri, Chen, & Wyslouzil, 2018). In the works of Chen, Siepmann, and co-workers (Kathmann et al., 2009), a combination of aggregation-volume-bias Monte Carlo, umbrella sampling, and histogram reweighting is applied to elucidate the structure and formation energy of the nucleating clusters. One finding of their work is that as the nucleating cluster grow in size, the shape of the cluster transitions from fractal-like to spherical (Chen, Siepmann, Oh, & Klein, 2002). Their work has also provided insight into the microheterogeneity (nonbulk-like mixing) of the nucleating clusters, e.g. core-shell structures and dumbbells (Nellas, Chen, & Ilja Siepmann, 2007). Through the construction of nucleation free energy surfaces, distinct nucleation pathways are identifiable in various combinations of nucleating vapors. For instance, in McKenzie and Chen (2006), binary nucleation of water-ethanol, water-nonane and ethanol-nonane are shown to follow different pathways: 1. water-ethanol vapors nucleate through the formation of mixed nuclei; 2. water-nonane vapors have two independent nucleation channels, with water or nonane enriched nuclei; 3. ethanol-nonane mixtures can nucleate through multiple nucleation pathways with varying cluster compositions. The nucleation energy surfaces for an ethanol-nonane system at 300 K and 360 K are shown in Figs. 2a and 2b, respectively, indicating that the formation free energy is similar for a range of cluster compositions.

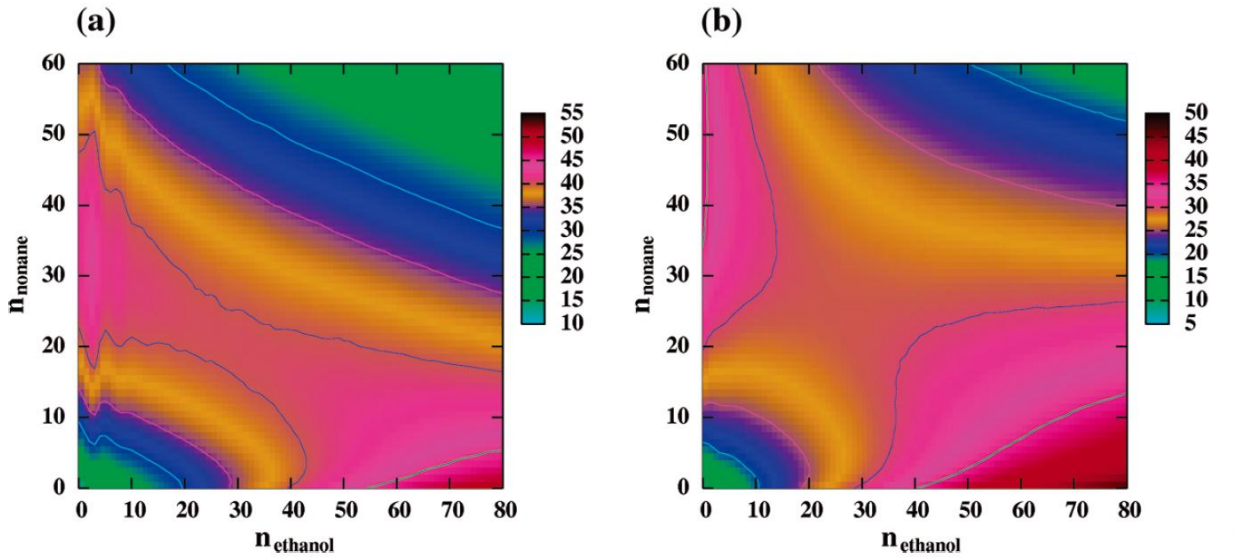

Fig 2. Contour plots for the nucleation free energy surface for a binary ethanol-nonane system at the following conditions (a) T = 300 K , $N_{nonane} = 1.7 \times 10^{-5}$ Å^{-3}, $N_{\mathrm{ethanol}} = 4.2 \times 10^{-6}$ Å^{-3} (b) T = 360 K, $N_{nonane} = 1.7 \times 10^{-5}$ Å^{-3}, $N_{\mathrm{ethanol}} = 3.8 \times 10^{-6}$ Å^{-3}. The color corresponds to cluster free energies of formation in units of k_BT. $n_{ethanol}$ and n_{nonane} are the numbers of ethanol and nonane molecules in the clusters, respectively. [Reprinted with permission from McKenzie & Chen (2006), *The Journal of Physical Chemistry*, 110, 3511-3516. Copyright 2006 American Chemical Society.]

Similar to MC, MD simulations can also be applied to simulate equilibrium cluster properties (Horsch, Vrabec, & Hasse, 2008; Julin, Napari, Merikanto, & Vehkamäki, 2008; Laasonen, Wonczak, Strey, & Laaksonen, 2000; Napari et al., 2009). Additionally, first-principles MD simulations have been applied to understand the formation and the stability of atmospheric relevant clusters (Loukonen et al., 2014a; Loukonen, Kuo, McGrath, & Vehkamäki, 2014b). However, MD is more powerful as a method to directly mimic gas-to-particle transitions, as introduced in the next section.

2.6 Molecular dynamics simulations

Through tracking down every atom in a simulation domain, MD simulations offer a way to directly simulate the highly dynamic nucleation processes. As MD uses force fields to describe atomic/molecular interactions, the mostly investigated nucleating species by MD are Lenard-Jones molecules, the simplicity of which help rule out complicating factors and speed up simulation (Angélil et al., 2014; Halonen et al., 2018; Napari et al., 2009; Salvalaglio, Tiwary, Maggioni, Mazzotti, & Parrinello, 2016; Tsai, Smith, & Tiwary, 2019; Zhukhovitskii, 2016). Another substance that has attracted a significant amount of attention is water (Angélil, Diemand, Tanaka, & Tanaka, 2015; Dumitrescu, Huinink, Smeulders, Dam, & Gaastra-Nedea, 2018; Dumitrescu, Smeulders, Dam, & Gaastra-Nedea, 2017; Duška, Němec, Hrubý, Vinš, & Planková, 2015; Matsubara et al., 2007; Tanaka, Kawano, & Tanaka, 2014; Yasuoka & Matsumoto, 1998b;

Zipoli et al., 2013). Metal, binary and ternary nucleation systems have also been investigated by MD (Braun, Kalikmanov, & Kraska, 2014; Braun & Kraska, 2012; Lümmen & Kraska, 2006; Römer & Kraska, 2007).

MD simulations come on different scales. Reliable nucleation statistics can either be extracted by many repetitions of nucleation in small-scale systems (a few hundred atoms), or fewer runs of large-scale systems (up to 10^9 atoms). Corresponding to the simulation scale, different methods are available to analyze the simulation results. For small-scale systems, the mean first-passage time (MFPT) method (Hänggi, Talkner, & Borkovec, 1990) is often employed to calculate nucleation rates. This method fits a three-parameter expression to the mean first passage time of k-mers, retrieving the nucleation time τ_J, the Zeldovich factor (Zeldovich, 1943), and the critical cluster size. The nucleation rate is then given by the inverse of the simulation domain volume multiplied by τ_J. For large-scale simulations, the Yasuoka–Matsumoto method (Yasuoka & Matsumoto, 1998a) is often applied. This method tracks the total number of clusters greater than threshold sizes, and the nucleation rate is given by derivatizing the cluster concentrations with respect to time. Chkonia, Wölk, Strey, Wedekind, and Reguera (2009) compared four methods to retrieve nucleation rates from MD simulations (the other two methods are the 'direct observation method' and the 'survival probability method'). They concluded that when applied properly, the nucleation rates derived from the four methods differ within a factor of two.

MD arguably provides the most comprehensive information of the nucleation process, as the distribution of nucleating cluster properties can be retrieved by taking snapshots of a fast-evolving nucleation system. These properties include cluster temperatures, density profiles, potential energies and shapes (Angélil et al., 2014; Ayuba, Suh, Nomura, Ebisuzaki, & Yasuoka, 2018; Wedekind, Reguera, & Strey, 2007). Take the cluster temperature distribution in a Lennard-Jones nucleation system (Angélil et al., 2014) as an example. Fig. 3a shows the temperature distribution of selected clusters from a single MD run, while Fig. 3b shows the ratio between the most probable cluster temperature and bath temperature as a function of cluster sizes for multiple MD runs. Fig. 3a clearly indicates that clusters of the same size have a non-Gaussian temperature distribution rather than a single, uniform temperature. This temperature distribution is fitted with the probability distribution function derived by McGraw and LaViolette (1995) (solid lines). Fig. 3b shows that although sub-critical clusters have most probable temperatures slightly lower than the bath temperature, post-critical clusters can retain much of the heat released upon argon phase transition, leading the temperature to rise well-above the bath temperature. This rise of cluster temperature as a function of cluster size is also discussed by Wedekind et al. (2007).

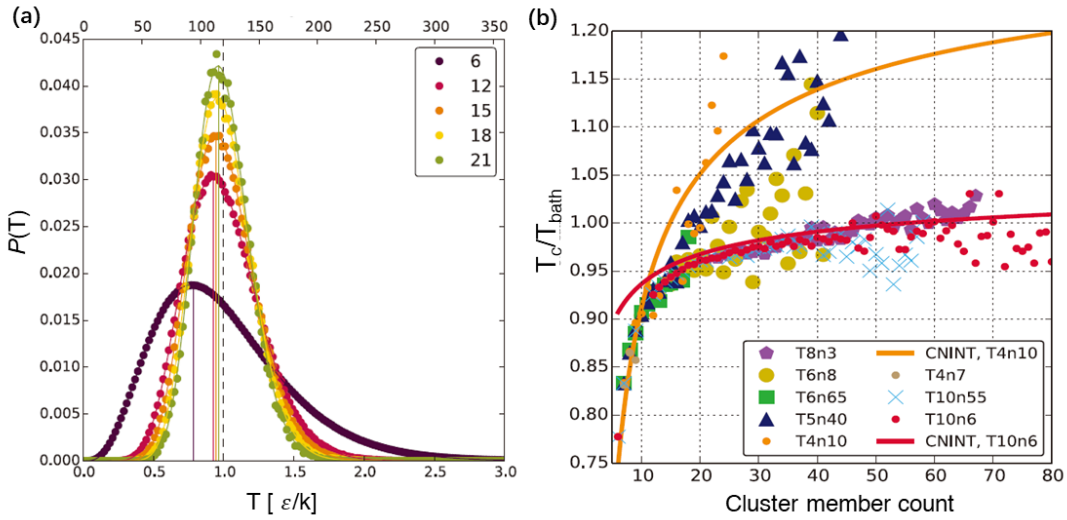

Fig. 3. (a) Temperature probability distributions (circles) for selected cluster sizes (see legend) in an MD nucleation simulation of Lennard-Jones molecules. The solid distribution curves are obtained through fitting the temperature distribution function proposed by McGraw and LaViolette (1995). The vertical solid lines indicate the most probable cluster temperature and the vertical dashed line shows the average bath temperature. (b) The ratio of the most probable cluster temperatures, T_C, to the bath temperature T_{bath}. The solid lines indicate the predictions from the classical non-isothermal theory (CNINT) from Feder et al. (1966) for runs T4n10 and T10n6. The labels indicate different MD simulation runs with in the format TXnY. X indicates system temperature and is equal to $10\times\frac{\epsilon}{k_B}$; Y indicates the concentration of the Lennard-Jones molecules at the beginning of the simulation (see Table 1 in the cited work for details). ϵ is the potential well depth in the Lennard-Jones model. [Reprinted from Angélil, R. et al. (2014) *Journal of Chemical Physics*, *140*, 074303-074303, with the permission of AIP Publishing]

With ease of scanning through simulation parameters, MD simulations facilitate tests of nucleation theories that are difficult to verify experimentally. One persisting problem in nucleation studies is the effect of carrier gas pressure and composition on nucleation rates, with literature reporting mixed evidences. Wedekind, Hyvärinen, Brus, and Reguera (2008) devised MD simulations to test their proposed mechanism on the effect of carrier gas pressure: higher carrier gas pressure increases nucleation rates by suppressing the non-isothermal effects, but decreases nucleation rates by adding extra volume work to the cluster formation process. They were able to vary the ratio between the carrier gas (helium) to the nucleating species (argon) from 1 to 20 in their MD simulations, which is hardly achievable by any given nucleation apparatus. Also dealing with the effect of carrier gas, Yasuoka and Zeng (2007) used carrier gas molecules with different interaction potentials in their simulations. They found that the effect of carrier gas pressure depends strongly on the potential model of the carrier gas molecules.

As a brute force method, MD simulation tracks the motion of every atom in the simulation domain, hence computational cost poses a major limit for MD applicability. Accurate simulation of atomic movements requires the time step used in MD to be a few femtoseconds, with the total simulation time

typically up to microseconds. Experimentally accessible nucleation rates of up to 10^{17} cm^{-3} s^{-1} (Wyslouzil & Wölk, 2016), once converted to the units more relevant for MD simulations, i.e. nm^{-3} μs^{-1}, are only 10^{-10} in value. This implies that nucleation is a truly 'rare' event from an MD perspective: to capture these events large simulation domains and long simulation times are needed. Limited by computational cost, most MD simulations use high supersaturation ratios to produce nucleation rates much higher than the experimentally accessible rates. Exceptions are the large-scale MD simulations performed by Tanaka and co-workers. For Lenard-Jones (LJ) systems, 10^8-10^9 atoms have been simulated for a time duration of up to 1.2 μs (Diemand, Angélil, Tanaka, & Tanaka, 2013). The scale of their simulation allows a nucleation rate as low as 10^{17} cm^{-3} s^{-1} to be achieved, overlapping with nucleation rates obtained from supersonic nozzles experiments (Sinha et al., 2010). For water nucleation, Angélil et al. (2015) performed the largest MD simulation so far: They simulated water nucleation containing 4×10^6 molecules, achieving a nucleation rate as low as 10^{19} cm^{-3} s^{-1}. Recently, Salvalaglio et al. (2016) proposed using Well Tempered Metadynamics to further extend the accessible nucleation rates by MD simulations. Using small scale simulations with only 512 argon molecules, their results are in quantitative agreement with nucleation rates from the aforementioned large scale simulations (Diemand et al., 2013). Very importantly, Salvalaglio et al. retrieved nucleation rates as low as 10^{13} cm^{-3} s^{-1}, showing great promise to perform parallel MD simulations and experiments that can be directly compared in future investigations.

A more nuanced aspect of MD simulations concerns the utilization of 'thermostats', which remove the latent heat released upon phase transition. Ideally, carrier gas should be used to remove heat from the nucleating clusters to mimic real experiments, but the incorporation of high-concentration carrier gas molecules incurs extra computational cost. Halonen et al. (2018) compiled MD-simulated nucleation rates from studies (Diemand et al., 2013; Napari et al., 2009; Tanaka, Tanaka, Yamamoto, & Kawamura, 2011; Wedekind et al., 2007) in which four thermostats (velocity scaling, Nose-Hoover, Berendsen, and stochastic Langevin) are applied. These rates were compared with reference rates assuming the clusters are fully thermalized, with cluster free energy determined from Monte-Carlo simulations. It is found that the MD-simulated nucleation rates are consistently lower than the MC-based rates. At low temperature, the deviation exceeds the non-isothermal effects predicted by Feder et al. (1966). This raises questions as to if an MD simulation with an artificial thermostat could represent a real nucleation experiment. A number of MD simulations have been performed using carrier gases as the thermostat (Wedekind et al., 2008; Wedekind et al., 2007; Yasuoka & Matsumoto, 1998b; Yasuoka & Zeng, 2007). However, to date there are no definitive guidelines as to the choice of thermostats or carrier gas concentrations. Systematic investigation on this front is still needed.

The application of MD simulations to atmospheric nucleation is very challenging. Compared with fundamental nucleation studies, atmospheric nucleation is characterized by even lower nucleation rates, making it extremely difficult to for MD to capture the nucleation events. Besides, MD simulation of atmospheric nucleation in general requires reactive force fields (Senftle et al., 2016) or even *ab initio* MD simulations to accurately simulate chemical reactions. *Ab initio* MD simulations of atmospheric nucleation are currently not feasible, but might come into reach as massive parallel Car-Parrinello type *ab initio* MD codes and computing infrastructures continue to develop.

3. Experimental measurements of nucleation

Experimental nucleation studies mainly belong in two categories: those that examine nucleation from a fundamental point of view (Wyslouzil & Wölk, 2016) and those that focus on nucleation relevant to Earth's atmosphere (Lee et al., 2019). In the former category, the nucleating vapors selected often have (relatively) simple molecular structures, i.e. water, CO_2, alkanes, alcohols, and noble gases. The concentrations of the nucleating vapors are usually known, hence the major experimental challenges to retrieve molecular level information are the successful detection of nucleating clusters and resolving nucleation dynamics within the experimental time scale. In the latter category, i.e. atmosphere-relevant nucleation studies, the time scale of nucleation is less of a concern (minutes to hours), but it is challenging to identify all the species that contribute to nucleation. Over the years, a wide range of techniques have been developed to understand nucleation of both categories, but not many directly provide molecular level information. In the following, we focus on two techniques that explicitly resolve nucleating cluster compositions and concentrations. The first one is controlled Laval expansion coupled with time-of-flight mass spectrometry, mainly applied in fundamental nucleation studies; the second is atmospheric pressure inlet-mass spectrometry, the current go-to technique for atmospheric nucleating cluster measurements. Other than these two techniques, direct experimental information of the nucleating clusters are not available, though constraining equations (e.g. heat and mass balance equations) can be applied to infer molecular cluster concentrations in some systems (Tanimura, Wyslouzil, & Wilemski, 2010). For a detailed account of other nucleation setups, we refer to reader to the excellent review by Wyslouzil and Wölk (2016).

3. 1 Nucleation in postnozzle flows of Laval expansions

Laval nozzles (or converging-diverging nozzles) allow gas expansion to proceed in a well-controlled manner with a strong cooling effect. The variation of pressure, temperature, gas speed inside the nozzle are known functions of nozzle geometries (Saad, 1985). This precise knowledge of gas properties makes Laval expansion suitable for nucleation studies. Wegener and co-workers were the first to study gas phase nucleation inside Laval nozzles (Wegener, 1975; Wegener & Wu, 1976). Later, Wyslouzil and co-

workers further developed this technique by incorporating a range of nucleation characterization techniques including pressure trace measurements, infra-red spectroscopy and small angle X-ray scattering (Ghosh et al., 2010; Khan, Heath, Dieregsweiler, Wyslouzil, & Strey, 2003; Pathak, Wölk, Strey, & Wyslouzil, 2014; Tanimura, Dieregsweiler, & Wyslouzil, 2010; Wyslouzil, Wilemski, Strey, Seifert, & Winans, 2007). Although molecular level information on the smallest nucleating cluster are not directly available, valuable information on nucleation rates, nucleated particle phase transition has been obtained with this method. An illustration of nucleation inside Laval nozzles is shown in Fig. 4a.

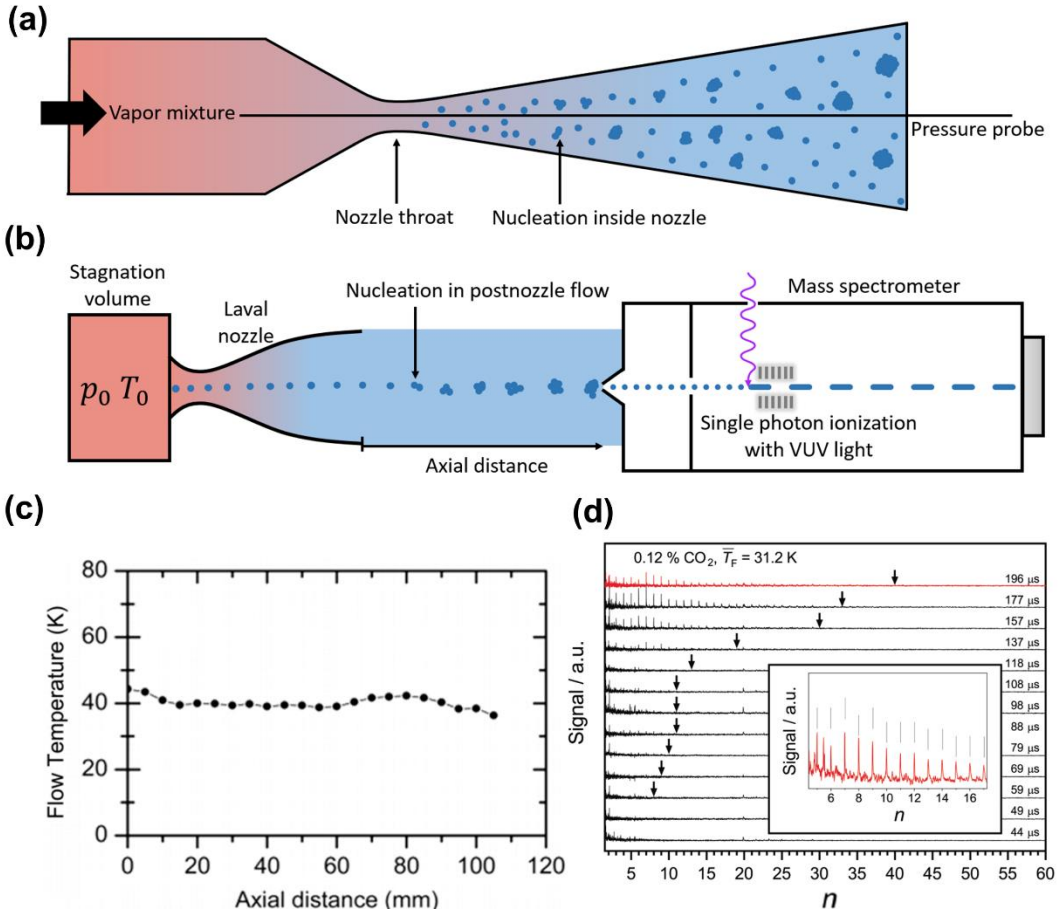

Fig. 4. (a) An illustration of gas phase nucleation inside Laval nozzles. The pressure probe is used to measure the gas pressure inside the nozzle, the deviation of which from theoretical values could inidicate a nucleation event. (b) A simplified schematic of the nucleation setup developed by Signorell and co-workers. See the text for a detailed explanation of its working principles. In both (a) and (b), the transition of color from red to blue indicates the drop in temperature of the carrier gas. (c) Flow temperature characterization in the axial direction of the postnozzle flow of the ETH setup. [Reprinted with permission from Schläppi et al. (2015), *Physcial Chemistry Chemical Physics*, *17* (39), 25761-25771–Published by the PCCP Owner Societies] (d) Cluster size distribution measured at different nucleation times (axial distances) during a CO_2 nucleation event. *n* is the number of molecules within the clusters; the black arrows indicate the position of the largest observable clusters. The inset plot is a zoomed-in spectrum of the uppermost trace. [Reprinted from

Krohn et al. (2020), *Physical Chemistry Chemical Physics, 22*(28), 15986-15998 – Published by the PCCP Owner Societies]

A recent, novel application of the Laval nozzle to nucleation studies does not induce nucleation inside the nozzle, but rather in a uniform postnozzle flow. The uniform postnozzle flow has previously found applications in chemical kinetics by several groups (Dupeyrat, Marquette, & Rowe, 1985; Lee, Hoobler, & Leone, 2000; Rowe, Marquette, & Rebrion, 1989), but its application to gas phase nucleation has been mainly explored with the Cinétique de Réaction en Ecoulement Supersonique Uniforme (CRESU) setup developed by Rowe and co-workers (Bourgalais et al., 2016; Sabbah, Biennier, Klippenstein, Sims, & Rowe, 2010), and the setup in ETH Zürich developed by Signorell and coworkers (Chakrabarty et al., 2017; Ferreiro, Chakrabarty, Schläppi, & Signorell, 2016; Li et al., 2019; Lippe et al., 2018; Lippe et al., 2019; Schläppi et al., 2015). Since the ETH setup is equipped with soft ionization techniques to better preserve cluster integrity (in contrast to electron impaction ionization used in the CRESU by Bourgalais et al. (2016)), in the following we use the setup schematic from the Signorell group (Fig. 4b) to demonstrate the working principles of this technique.

In a typical experiment, one or more nucleating vapors along with a carrier gas (usually nitrogen, argon and their mixtures) is supplied to the stagnation volume (red shaded area) of a Laval nozzle with pulsed valves. As the gas expands through nozzle, the flow speed increases while the flow temperature and pressure quickly drop (the temperature drop is indicated by the color shift from red to blue in Fig. 4b), leading to supersaturations of the nucleating vapors. By matching the chamber pressure to the flow pressure at the nozzle exit, the postnozzle flow achieves and maintains uniformity in speed, temperature, and pressure within a ~10 cm distance. This is in contrast to a free gas expansion process with strong spatial gradients of flow properties. The flow uniformity is the key to nucleation experiments, not only because nucleation is extremely sensitive to ambient conditions, but also because flow uniformity guarantees that the nucleation-related rate constants remain the same in the postnozzle region, enabling detailed kinetic analysis. Fig. 4c illustrates the flow uniformity by showing the temperature fluctuations as a function of the axial distance (Schläppi et al., 2015). The nucleating clusters formed in the postnozzle flow are sampled by a skimmer that connects to a differential chamber at 10^{-5} Pa, and are then directed into a time-of-flight chamber at 10^{-7} Pa, where the clusters are ionized by single photon ionization with a vacuum ultraviolet (VUV) laser (Belau, Wilson, Leone, & Ahmed, 2007; Chakrabarty et al., 2017; Litman et al., 2013). We note that the clusters remain neutral until they are ionized in a collision-less, low pressure environment. This avoids collision-induced dissociation (CID) of the ionized clusters in ion optics (compare to the APi-Tof introduced in the next section). With the combination of VUV ionization and lack of CID, the integrity of weakly-bound clusters is well-preserved. The laser-ionized clusters are then extracted by an electrostatic

lens and detected by a microchannel plate. To increases instrument sensitivity, the voltage applied to the electrostatic lens is up to 30 kV.

To capture the temporal variation of the cluster size distributions in the nucleation process, the distance between the nozzle exit and the skimmer is adjustable by mounting the Laval nozzle on a translation stage. At constant flow speed, the distance between the nozzle-exit and the skimmer translates to nucleation time, and the allowable time resolution is down to ~2 μs. As an example, Fig. 4d shows CO_2 cluster size distributions at different nucleation times measured at 31.2 K and a CO_2 percentage of 0.12% (Krohn et al., 2020). By adding a gas standard such as CH_4 with known photoionization cross section into the carrier gas, the absolute concentration of each detectable cluster can be quantified by the following equation,

$$N_n^{\mathrm{a}} = \frac{I_n}{I^s}\frac{\sigma^s}{n\cdot\sigma^a}\cdot N^s \tag{16}$$

where N_n stands for the number concentration of clusters containing n monomers, I for the ion signal and σ for the molecular photoionization cross section. The superscripts 'a' and 's' stand for 'analyte' and 'standard', respectively.

Through the combination of the above techniques, weakly-bound clusters can be detected and quantified, with their temporal variations resolved. To date, the Laval-based setups have provided unprecedented details on the unary homogeneous nucleation of propane (Ferreiro et al., 2016; Schläppi et al., 2015), toluene (Chakrabarty et al., 2017), water (Bourgalais et al., 2016; Li et al., 2019; Lippe et al., 2018) and CO_2 (Krohn et al., 2020; Lippe et al., 2019). Apart from the quantities available from conventional nucleation measurements, e.g. onset conditions of nucleation and the nucleation rates, the time-resolved cluster size distributions enable the determination of dimerization rate constants and monomer-cluster association rate constants (Li et al., 2019; Lippe et al., 2018). The extracted rate constants further allow direct comparison between experiments and calculations based on first principles (Bourgalais et al., 2016; Sabbah et al., 2010). By changing nozzle geometries and carrier gas compositions, the relative magnitude of the monomer association rate and cluster evaporation rate can also be measured as a function of temperature, providing evidence of shifting nucleation barrier heights as temperature varies (Krohn et al., 2020).

Despite its great potential to unveil the nucleation process on the molecular level, currently there are a few limiting factors for this Laval-based technique. First, even though single photon ionization is in general a soft ionization technique, it still leads to composition-dependent cluster fragmentation and intra-cluster chemistry. Water clusters may only lose a monomer upon single photon ionization (Belau et al.,

2007; Litman et al., 2013), but intra-cluster chemical reactions can follow ionization for other species, e.g. dimethyl ether and acids (Litman et al., 2013). Second, to date nucleation experiments with the Laval-based setups have been limited to low-temperatures (under 100 K). While this temperature range is advantageous for understanding nucleation by weakly-interacting species, substances with stronger intermolecular interactions, e.g. those of atmospheric relevance, may not exhibit nucleation behavior of interest. To study nucleation of these substances, the accessible temperature of the postnozzle flow need to be expanded.

3.2 Detection of nucleating clusters at atmospheric conditions

Atmospheric nucleation (or new particle formation, NPF) is the most extensively studied nucleation phenomenon because of its influence on the climate, on human health and its inherent complexity (Chu et al., 2019; Gordon et al., 2017; Guo et al., 2014; Kazil et al., 2010; Lee et al., 2019; Merikanto et al., 2009; Spracklen et al., 2008; Wang et al., 2017; Zhang, Khalizov, Wang, Hu, & Xu, 2012). Elucidation of the NPF mechanisms is a twofold problem that entails (a) identification and quantification of the nucleating vapors and ions in the atmosphere (Johnston & Kerecman, 2019; Junninen et al., 2010; Mirme & Mirme, 2013; Zhao, 2018), and (b) determination of the chemical composition and concentration of the nucleating clusters. Here we focus on the latter and look into the instruments that are the work horses for detection of atmospheric nucleating clusters, i.e. the Cluster-CIMS and (CI)-APi-TOF.

Nucleating clusters formed in atmospheric nucleation events are both low in concentration and fragile, hence the detection and quantification of these clusters demand not only high instrument sensitivity, but also cluster integrity being preserved to a good extent. Eisele and co-workers (Ball, Hanson, Eisele, & McMurry, 1999; Eisele & Hanson, 2000; Eisele & Tanner, 1993; Hanson & Eisele, 2002) were the first to explore utilizing chemical ionization to detect atmospherically-relevant, neutral nucleating clusters and laid the ground for the current detection methods. They carried out mass spectrometric analysis of nucleating vapors and clusters, preceded by analyte chemical ionization with nitrate ions at atmospheric pressure. Ionization in the atmosphere is essential to avoid dilution of the nucleating clusters, and chemical ionization with nitrate ions ensures that the ionization process is ‘soft’ to minimize cluster fragmentation. The prototype instrument used in their works later evolved into the Cluster-CIMS, i.e. cluster chemical ionization mass spectrometer (Chen et al., 2012; Jen, Bachman, Zhao, McMurry, & Hanson, 2016a; Jen et al., 2014; Jen, Zhao, McMurry, & Hanson, 2016b; Jiang et al., 2011; Zhao, Eisele, Titcombe, Kuang, & McMurry, 2010; Zhao et al., 2011). Fig. 5a shows a schematic of this instrumentation consisting of (from the left to the right) the ionization source, the atmospheric pressure interface, an octupole to facilitate ion transmission, a quadrupole for ion separation and an ion detector. Nitrate ions are produced by passing trace amounts of nitric acid vapors nearby a radioactive source, with chemical ionization taking place in either a

flow tube operation mode or a traverse ion operation mode (the mode is unspecified in Fig. 5a) following the reaction schemes:

$$XH + (HNO_3)_n NO_3^- \rightarrow X^- + (HNO_3)_n HNO_3, \text{(R1)}$$

$$XH + (HNO_3)_n NO_3^- \rightarrow XH \cdot NO_3^- + (HNO_3)_n. \text{(R2)}$$

R1 indicates ionization by proton transfer reaction and R2 indicates ionization by adduct formation. By changing the chemical ionization reaction time, reagent ion-induced cluster formation and the original neutral clusters can be distinguished (Eisele & Hanson, 2000; Zhao et al., 2010).

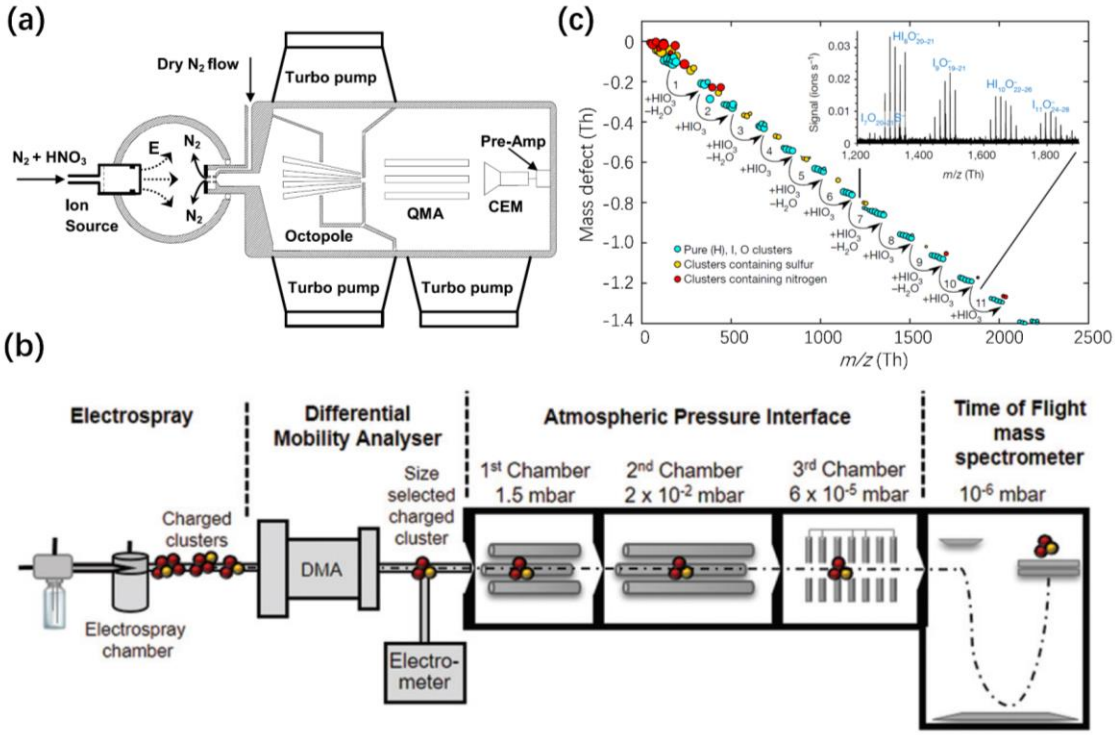

Fig. 5. (a) The instrument schematic of the Cluster-CIMS developed by Zhao et al. [Reprinted with permission from Zhao et al. (2010), *Journal of Geophysical Research: Atmospheres, 115*(D8). Copyright 2010 by the American Geophysical Union] (b) An illustrative instrument schematic of the APi-Tof. A cluster generation setup is connected to the front of the APi to produce clusters of known compositions to facilitate instrument calibration. The APi consists of three chambers with sequentially decreasing pressures, with the third chamber connected to the time-of-flight chamber. [Reprinted with permission from Passananti et al. (2019), *Chemical Communications, 55*(42), 5946-5949 – Published by The Royal Society of Chemistry] (c) CI-APi-Tof measured mass defect plot as a function of cluster mass-to-charge ratio (*m/z*) during a nucleation event initiated by HIO_3. The clusters are hypothesized to form via sequential addition of HIO_3. The area of the symbols are proportional to the observed signal. The inset plot is a portion of the recorded raw mass spectrum. Refer to the cited work for chemical reactions of 1-11. [Adpated with permission by Springer Nature: *Nature*, Molecular-scale evidence of aerosol particle formation via sequential addition of HIO_3, Sipilä et al. (2016). Copyright 2016]

The application of cluster-CIMS to atmospheric field measurements marked an important step in detecting atmospheric neutral clusters (Chen et al., 2012; Jiang et al., 2011; Zhao et al., 2010). However, the Cluster-CIMS uses a quadrupole to separate charged clusters and only has unit-mass resolution, which is insufficient to fully resolve the exact molecular content of the nucleating clusters. This limitation was lifted through coupling time-of-flight spectrometry (Tof), chemical ionization (CI) and an atmospheric pressure inlet (APi), i.e. the CI-APi-Tof (Jokinen et al., 2012). Without the chemical ionization inlet, the CI-APi-Tof reduces to an APi-Tof (Junninen et al., 2010), which is suitable for the detection of naturally charged nucleating species and ion-induced nucleation (Duplissy et al., 2016; Kirkby et al., 2016). Fig. 5b shows a schematic of the APi-Tof connected to a cluster-generation setup used for instrument calibration. The (CI-)APi-Tof has a resolving power between 3000 and 7000 m/z, enabling it to determine the exact molecular composition of neutral nucleating clusters. The mass-spectrometric data retrieved from (CI-)API-Tof measurements are usually presented as mass defect plots, as demonstrated in Fig. 5c. With the (CI-)APi-Tof, a wide range of atmospheric nucleating clusters have been identified, including but not limited to sulfuric acid-amines/ammonia-oxidized organics clusters (Almeida et al., 2013; Kürten et al., 2014; Riccobono et al., 2014; Yao et al., 2018), iodine oxoacids and iodine oxide clusters (Sipilä et al., 2016) and clusters containing only ions and highly oxidized molecules (Frege et al., 2018; Kirkby et al., 2016). These works in total suggest that sulfuric acid is a necessary ingredient for atmospheric nucleation, with water, ammonia/amines, and organics facilitating the nucleation process. Exceptions are the nucleation in coastal regions, which could mainly involve iodine containing clusters, and ion induced nucleation, which does not require the presence of sulfuric acid.

The Cluster-CIMS and (CI-)APi-TOF are the current go-to techniques for the detection of atmospheric clusters (especially the latter). Recently, Riva et al. (2019) coupled atmospheric CI with an orbitrap, which further increases the instrument resolution (up to 140,000 at m/z = 200) and allows tandem mass spectrometry to elucidate molecular structures. Since CI-Orbitrap is yet to be widely applied in nucleation studies, in the following we shall classify the significant amount of effort that has been devoted to the characterizations of Cluster-CIMS and (CI-)APi-TOF:

a. Mass dependent transmission efficiency. By comparing the signal of the Cluster-CIMS to that of an electrometer, Zhao et al. (2010) showed that the ion transmission efficiency in the Cluster-CIMS is ion mass dependent and is a function of the applied frequency to the octupole. Their calibration setup is similar to the one presented in Fig. 5b, i.e. using calibration ions produced by electrospray and selected by an high resolution differential mobility analyzer (Rosser & de la Mora, 2005). A similar calibration procedure is

reported for the APi-Tof (Junninen et al., 2010). Heinritzi et al. (2016) incorporated the ionization step into the mass dependency calibration by adding perfluorinated acids to deplete primary nitrate ions. They showed that there is a non-negligible mass discrimination effect in the CI source: the relative transmission efficiency increases by a factor around 5 as m/z of the ions increase from 62 to 550. This mass dependency is applied in recent atmospheric nucleation and growth measurements to correct the raw data (Stolzenburg et al., 2018).

b. Ionizing Reagents. To date, the detection of atmospheric nucleating clusters has mostly been accomplished with nitrate ions as the ionizing reagent ions. Nitrate ions have shown good sensitivity for sulfuric-acid containing clusters, but its charging efficiency is composition dependent and low for less oxidized species (Rissanen, Mikkilä, Iyer, & Hakala, 2019). Compared to nitrate ions, acetate ions allow detection with higher efficiency (Berndt et al., 2016; Berndt et al., 2015), but acetate ionization chemistry is more complex, characterized by a broader range of ionizing clusters that are strongly influenced by relative humidity (Brophy & Farmer, 2016). Because of these complicating factors, acetate ions have seen limited applications in cluster detection (Jen, Hanson, & McMurry, 2015; Jen et al., 2016b). Other ionizing reagents, including iodide ions (Iyer, Lopez-Hilfiker, Lee, Thornton, & Kurtén, 2016) and bisulfate ions (Sipilä et al., 2015), are mainly used for detecting gaseous species instead of molecular clusters. Since different ions have varying sensitivities and compound selectivity, instruments that feature switchable ionization schemes have the potential to provide a more complete picture of nucleation pathways (Brophy & Farmer, 2015; Rissanen et al., 2019). Besides experimental characterization, our understanding of ionization chemistry is also facilitated by quantum chemistry computations of ion-neutral binding energies (Hyttinen et al., 2018; Hyttinen, Rissanen, & Kurtén, 2017; Iyer et al., 2016).

c. Cluster transformation upon ionization. Even though chemical ionizations are relatively soft, clusters are likely to go through composition transformation upon ionization. Ortega et al. (2014) calculated the evaporation rates of charged sulfuric acid-base clusters and found that negative charging will lead to the increase of sulfuric-acid: base ratios, while positive charging will decrease the ratio. It has also been shown that charged sulfuric acid clusters are less hydrated than their neutral counterparts (Ehrhart et al., 2016); this could contribute to water evaporation upon ionization of sulfuric acid clusters.

d. Collision-induced dissociation. Upon entrance into the APi, clusters ionized at the atmospheric pressure are accelerated at reduced pressures by the ion optics, which leads to collision-induced cluster fragmentation. Passananti et al. (2019) experimentally measured and simulated the fragmentation of $(H_2SO_4)_2HSO_4^-$ in an APi-Tof. The experimental setup is shown in Fig. 5b. They found that the voltage configuration of the second chamber in the APi has the strongest influence on $(H_2SO_4)_2HSO_4^-$ fragmentation. In the first chamber, the clusters do not accumulate enough kinetic energy in between collisions with carrier

gas molecules to induce fragmentation, while in the third chamber the clusters rarely collide with carrier gas molecules because of the low pressure. No voltage configurations of the ion optics would eliminate fragmentation of $(H_2SO_4)_2HSO_4^-$, but some configurations lead to complete fragmentation of the cluster. Leiminger et al. (2019) used hexapoles in lieu of quadrupoles to decrease cluster fragmentation during transmission. With the $H_3O^+(H_2O)_{n=0-3}$ model system, they estimated clusters with binding energies higher than 19 kcal mol^{-1} can be transmitted through the APi without significant fragmentation. This is lower than a previously reported value of 25 kcal mol^{-1} for quadrupole-based instruments (Iyer et al., 2016). Currently, thorough characterization of collision-induced fragmentation of atmospherically relevant clusters is still limited, but in the future the simulation framework developed by Vehkamäki and coworkers (Passananti et al., 2019; Zanca et al., 2020; Zapadinsky et al., 2019) can be utilized to estimate cluster survival ratios.

e. Calibration factor. With proper calibration standards, a calibration factor for a given analyte can be empirically obtained for an instrument setting, which encompasses all the factors (a-d) mentioned above and converts measured signals to analyte concentrations. For CI-APi-Tof measurements, the calibration factor for sulfuric acid monomer is derived from measurements using a well-characterized H_2SO_4 generator (Kürten, Rondo, Ehrhart, & Curtius, 2012). For most highly oxygenated molecules (HOMs), however, authentic calibration standards are not available, hence the quantification of HOMs are achieved by using the same calibration factor as sulfuric acid molecules (Berndt et al., 2015; Lehtipalo et al., 2018; Tröstl et al., 2016), or determined with a surrogate molecule with a gravimetrically calibrated permeation source (Ehn et al., 2014). This is a major source of uncertainty for CI-APi-Tof data, especially for compounds that may exhibit lower levels of ionization efficiency (Berndt et al., 2016; Berndt et al., 2015; Hyttinen et al., 2015; Hyttinen et al., 2018; Hyttinen et al., 2017). For nucleating clusters, although studies have indicated that detection efficiency is cluster composition and instrument-setting dependent (Kürten et al., 2014; Passananti et al., 2019), calibration standards are not available.

f. Missing hydrated clusters. Theoretical and experimental evidence suggests that under atmospheric conditions, the nucleating clusters are hydrated (Ahonen et al., 2019; Hanson & Lovejoy, 2006; Henschel et al., 2016; Henschel et al., 2014; Kildgaard et al., 2018a; Thomas et al., 2016). However, for both the Cluster-CIMS and (CI-)APi-Tof, water molecules quickly evaporate from the clusters once they enter the mass spectrometer since the atmospheric hydration equilibrium is no longer maintained. This is even the case for binary sulfuric-water nucleation in which water definitively participates in the nucleation process (Eisele & Hanson, 2000). The loss of water makes it difficult to directly examine the role of water in the atmospheric nucleation process.

g. Comparison with measurements of nucleated particles. The molecular level information obtained by either the Cluster-CIMS or the (CI-)APi-Tof needs to be compared with other established methods for the

detection of nanometer range nucleated particles (Kangasluoma et al., 2020). Jen et al. (2015) compared the particle number concentrations predicted based on Cluster-CIMS measurements and those measured by a scanning mobility particle spectrometer equipped with a diethylene glycol condensation particle counter (DEG-SMPS). Good agreement was achieved except at low sulfuric acid concentrations. However, studies on the reconciliation between molecular level measurements and particle level measurements are still lacking.

As detailed above, although atmospheric nucleating clusters can be detected by the Cluster-CIMS and (CI-)APi-Tof, there exists a level of uncertainty in data interpretation, especially when it comes to quantification of the nucleating clusters. Further systematic and innovative work is needed to constrain experimental uncertainties caused by cluster fragmentation and variable ionization efficiency. The identification of nucleating clusters, the composition of which correspond to different nucleation pathways, is an ongoing effort: The existing research works cannot rule out the possibility that a subset of atmospheric trace species, similar to water, participate in atmospheric nucleation but are hitherto unidentified in nucleating clusters. These species may cluster with low-volatility species such as sulfuric acid in the atmosphere and enhance nucleation, but the clusters are relatively weakly bound and severely fragment inside the detection instrument. With existing experimental setups (i.e. flow reactors, smog chambers) robust experiments can be devised to identify species that enhance nucleation (Arquero, Gerber, & Finlayson-Pitts, 2017; Perraud, Xu, Gerber, & Finlayson-Pitts, 2020; Yu, McGraw, & Lee, 2012; Zhang et al., 2004). Future improvement of instrumentation should aim at reconciling observed nucleating clusters and nucleation enhancement measurements.

4. Summary and Outlook

In this review, we summarized the techniques to probe nucleation on the molecular level. The introduced modeling methods facilitate the interpretation of the experimental data and give insight into the nucleation process. In particular,

- GDE-based kinetic simulations are routinely applied to understand atmospheric nucleation (the critical rates in the model are often obtained by QC calculations). GDE-based kinetic simulations work best for simulating nucleation when the major nucleation participants are known. Molecular level information retrieved from the Laval-based experiments have also been analyzed by GDE-based kinetic simulations.
- QC calculations are extremely valuable in evaluating cluster stability. This helps identify/rule out nucleation participants. Some well-controlled nucleation experiments, e.g. sulfuric acid-water binary nucleation studies in the CLOUD chamber, are nicely explained by QC-based theories. QC also

facilitates constraining experimental uncertainties in terms of analyte dissociation, hydration, and ionization.

However, as explained in this review, each method has its limitations, hence the task of improving individual techniques and bringing modeling and experiments together to characterize nucleation requires continued efforts. For future scientific endeavors in gas phase nucleation, we believe the following general directions may be considered:

- For GDE-based kinetic simulations, further development should focus on efficient simulation of more complex systems, with user-friendly interfaces to large quantum mechanical cluster energy databases. Coupling of the GDE with gas phase chemistry, multi-phase chemistry should facilitate simulating the entire evolution of atmospheric particles.
- For molecular dynamics simulations, recent developments (Diemand et al., 2013; Salvalaglio et al., 2016) have shown the possibility to reach a true overlap between simulated nucleation rates and experimental nucleation rates. Joint efforts between experimental and modelling groups are in need to implement direct comparison between experimental and simulation data. Development of guidelines for simulations, e.g. the proper choice of thermostats, is needed.
- For nucleation measurements in the postnozzle flow of Laval nozzles, multicomponent nucleation pathways are yet to be fully explored. Expanding the accessible temperature range by the postnozzle flow should open the door to more nucleation systems of interest and facilitate comparison with results measured with other experimental techniques.
- For the measurement of atmospherically relevant nucleating clusters, efforts to constrain the uncertainties in cluster detection and quantifications are still much needed. Minimizing cluster fragmentation may help reveal unidentified nucleation pathways.

Acknowledgements

This work was supported by the Swiss National Science Foundation (project nr. 200020_172472) and ETH Zurich.

About this Article

The article is an editor-invited review article. Editor-Invited review articles began in 2020 to commemorate the 50th anniversary of the Journal of Aerosol Science.

Declaration of competing interest

The authors declare no competing interest。

References

Ahmad, M., Casey, M., & Sürken, N. (2009). Experimental assessment of droplet impact erosion resistance of steam turbine blade materials. *Wear, 267*(9), 1605-1618.

Ahonen, L., Li, C., Kubečka, J., Iyer, S., Vehkamäki, H., Petäjä, T., . . . Hogan Jr, C. J. (2019). Ion Mobility-Mass Spectrometry of Iodine Pentoxide–Iodic Acid Hybrid Cluster Anions in Dry and Humidified Atmospheres. *The Journal of Physical Chemistry Letters, 10*(8), 1935-1941.

Almeida, J., Schobesberger, S., Kürten, A., Ortega, I. K., Kupiainen-Määttä, O., Praplan, A. P., . . . Kirkby, J. (2013). Molecular understanding of sulphuric acid–amine particle nucleation in the atmosphere. *Nature, 502*, 359.

Angélil, R., Diemand, J., Tanaka, K. K., & Tanaka, H. (2014). Properties of liquid clusters in large-scale molecular dynamics nucleation simulations. *The Journal of Chemical Physics, 140*, 074303-074303.

Angélil, R., Diemand, J., Tanaka, K. K., & Tanaka, H. (2015). Homogeneous SPC/E water nucleation in large molecular dynamics simulations. *The Journal of chemical Physics, 143*, 064507-064507.

Arquero, K. D., Gerber, R. B., & Finlayson-Pitts, B. J. (2017). The Role of Oxalic Acid in New Particle Formation from Methanesulfonic Acid, Methylamine, and Water. *Environmental Science & Technology, 51*(4), 2124-2130.

Ayuba, S., Suh, D., Nomura, K., Ebisuzaki, T., & Yasuoka, K. (2018). Kinetic analysis of homogeneous droplet nucleation using large-scale molecular dynamics simulations. *The Journal of Chemical Physics, 149*(4), 044504.

Ball, S. M., Hanson, D. R., Eisele, F. L., & McMurry, P. H. (1999). Laboratory studies of particle nucleation: Initial results for H2SO4, H2O, and NH3 vapors. *Journal of Geophysical Research: Atmospheres, 104*(D19), 23709-23718.

Becker, R., & Döring, W. (1935). Kinetische Behandlung der Keimbildung in übersättigten Dämpfen. *Annalen der Physik, 416*(8), 719-752.

Belau, L., Wilson, K. R., Leone, S. R., & Ahmed, M. (2007). Vacuum Ultraviolet (VUV) Photoionization of Small Water Clusters. *The Journal of Physical Chemistry A, 111*, 10075-10083.

Berndt, T., Richters, S., Jokinen, T., Hyttinen, N., Kurtén, T., Otkjær, R. V., . . . Ehn, M. (2016). Hydroxyl radical-induced formation of highly oxidized organic compounds. *Nature Communications, 7*(1), 13677.

Berndt, T., Richters, S., Kaethner, R., Voigtländer, J., Stratmann, F., Sipilä, M., . . . Herrmann, H. (2015). Gas-Phase Ozonolysis of Cycloalkenes: Formation of Highly Oxidized RO_2 Radicals and Their Reactions with NO, NO_2, SO_2, and Other RO_2 Radicals. *The Journal of Physical Chemistry A, 119*(41), 10336-10348.

Bork, N., Elm, J., Olenius, T., & Vehkamäki, H. (2014). Methane sulfonic acid-enhanced formation of molecular clusters of sulfuric acid and dimethyl amine. *Atmospheric Chemistry and Physics, 14*(22), 12023-12030.

Bourgalais, J., Roussel, V., Capron, M., Benidar, A., Jasper, A. W., Klippenstein, S. J., . . . Le Picard, S. D. (2016). Low Temperature Kinetics of the First Steps of Water Cluster Formation. *Physical Review Letters, 116*, 113401-113401.

Bowles, R. K., McGraw, R., Schaaf, P., Senger, B., Voegel, J. C., & Reiss, H. (2000). A molecular based derivation of the nucleation theorem. *The Journal of Chemical Physics, 113*(11), 4524-4532.

Braun, S., Kalikmanov, V., & Kraska, T. (2014). Molecular dynamics simulation of nucleation in the binary mixture n-nonane/methane. *The Journal of Chemical Physics, 140*(12), 124305.

Braun, S., & Kraska, T. (2012). Dynamic structure of methane/n-nonane clusters during nucleation and growth. *The Journal of Chemical Physics, 136*(21), 214506.

Bromley, S. T., Gómez Martín, J. C., & Plane, J. M. C. (2016). Under what conditions does $(SiO)_N$ nucleation occur? A bottom-up kinetic modelling evaluation. *Physical Chemistry Chemical Physics, 18*(38), 26913-26922.

Brophy, P., & Farmer, D. K. (2015). A switchable reagent ion high resolution time-of-flight chemical ionization mass spectrometer for real-time measurement of gas phase oxidized species: characterization from the 2013 southern oxidant and aerosol study. *Atmospheric Measurement Techniques, 8*(7), 2945-2959.

Brophy, P., & Farmer, D. K. (2016). Clustering, methodology, and mechanistic insights into acetate chemical ionization using high-resolution time-of-flight mass spectrometry. *Atmospheric Measurement Techniques, 9*(8), 3969-3986.

Brus, D., Hyvärinen, A.-P., Ždímal, V., & Lihavainen, H. (2005). Homogeneous nucleation rate measurements of 1-butanol in helium: A comparative study of a thermal diffusion cloud chamber and a laminar flow diffusion chamber. *The Journal of Chemical Physics, 122*(21), 214506.

Cai, R., Chandra, I., Yang, D., Yao, L., Fu, Y., Li, X., . . . Jiang, J. (2018). Estimating the influence of transport on aerosol size distributions during new particle formation events. *Atmospheric Chemistry and Physics, 18*(22), 16587-16599.

Carlsson, P. T. M., Celik, S., Becker, D., Olenius, T., Elm, J., & Zeuch, T. (2020). Neutral Sulfuric Acid–Water Clustering Rates: Bridging the Gap between Molecular Simulation and Experiment. *The Journal of Physical Chemistry Letters, 11*(10), 4239-4244.

Carlsson, P. T. M., & Zeuch, T. (2018). Investigation of nucleation kinetics in H2SO4 vapor through modeling of gas phase kinetics coupled with particle dynamics. *The Journal of Chemical Physics, 148*(10), 104303.

Chakrabarty, S., Ferreiro, J. J., Lippe, M., & Signorell, R. (2017). Toluene Cluster Formation in Laval Expansions: nucleation and Growth. *J. Phys. Chem. A, 121*, 3991-4001.

Chen, B., Siepmann, J. I., & Klein, M. L. (2003). Simulating the Nucleation of Water/Ethanol and Water/n-Nonane Mixtures: Mutual Enhancement and Two-Pathway Mechanism. *Journal of the American Chemical Society, 125*(10), 3113-3118.

Chen, B., Siepmann, J. I., Oh, K. J., & Klein, M. L. (2001). Aggregation-volume-bias Monte Carlo simulations of vapor-liquid nucleation barriers for Lennard-Jonesium. *The Journal of Chemical Physics, 115*(23), 10903-10913.

Chen, B., Siepmann, J. I., Oh, K. J., & Klein, M. L. (2002). Simulating vapor–liquid nucleation of n-alkanes. *The Journal of Chemical Physics, 116*(10), 4317-4329.

Chen, H., Ezell, M. J., Arquero, K. D., Varner, M. E., Dawson, M. L., Gerber, R. B., & Finlayson-Pitts, B. J. (2015). New particle formation and growth from methanesulfonic acid, trimethylamine and water. [10.1039/C5CP00838G]. *Physical Chemistry Chemical Physics, 17*(20), 13699-13709.

Chen, M., Titcombe, M., Jiang, J., Jen, C., Kuang, C., Fischer, M. L., . . . McMurry, P. H. (2012). Acid–base chemical reaction model for nucleation rates in the polluted atmospheric boundary layer. *Proceedings of the National Academy of Sciences, 109*(46), 18713.

Chkonia, G., Wölk, J., Strey, R., Wedekind, J., & Reguera, D. (2009). Evaluating nucleation rates in direct simulations. *The Journal of Chemical Physics, 130*(6), 064505.

Chu, B., Kerminen, V. M., Bianchi, F., Yan, C., Petäjä, T., & Kulmala, M. (2019). Atmospheric new particle formation in China. *Atmospheric Chemistry and Physics, 19*(1), 115-138.

Daum, F. L. (1963). AIR CONDENSATION IN A HYPERSONIC WIND TUNNEL. *AIAA Journal, 1*(5), 1043-1046.

Diemand, J., Angélil, R., Tanaka, K. K., & Tanaka, H. (2013). Large scale molecular dynamics simulations of homogeneous nucleation. *The Journal of Chemical Physics, 139*, 074309-074309.

Du, H., Nadykto, A. B., & Yu, F. (2009). Quantum-mechanical solution to fundamental problems of classical theory of water vapor nucleation. *Physical Review E, 79*(2), 021604.

Dumitrescu, L. R., Huinink, H., Smeulders, D. M. J., Dam, J. A. M., & Gaastra-Nedea, S. V. (2018). Water nucleation in helium, methane, and argon: A molecular dynamics study. *The Journal of Chemical Physics, 148*(19), 194502.

Dumitrescu, L. R., Smeulders, D. M. J., Dam, J. A. M., & Gaastra-Nedea, S. V. (2017). Homogeneous nucleation of water in argon. Nucleation rate computation from molecular simulations of TIP4P and TIP4P/2005 water model. *The Journal of Chemical Physics, 146*(8), 084309.

Dunne, E. M., Gordon, H., Kürten, A., Almeida, J., Duplissy, J., Williamson, C., . . . Carslaw, K. S. (2016). Global atmospheric particle formation from CERN CLOUD measurements. *Science, 354*(6316), 1119.

Dupeyrat, G., Marquette, J. B., & Rowe, B. R. (1985). Design and testing of axisymmetric nozzles for ion–molecule reaction studies between 20 °K and 160 °K. *The Physics of Fluids, 28*(5), 1273-1279.

Duplissy, J., Merikanto, J., Franchin, A., Tsagkogeorgas, G., Kangasluoma, J., Wimmer, D., . . . Kulmala, M. (2016). Effect of ions on sulfuric acid-water binary particle formation: 2. Experimental data and comparison with QC-normalized classical nucleation theory. *Journal of Geophysical Research: Atmospheres, 121*(4), 1752-1775.

Duška, M., Němec, T., Hrubý, J., Vinš, V., & Planková, B. (2015). Molecular dynamics simulation of vapour-liquid nucleation of water with constant energy. *EPJ Web Conf., 92*, 02013-02013.

Ehn, M., Thornton, J. A., Kleist, E., Sipilä, M., Junninen, H., Pullinen, I., . . . Mentel, T. F. (2014). A large source of low-volatility secondary organic aerosol. *Nature, 506*, 476.

Ehrhart, S., & Curtius, J. (2013). Influence of aerosol lifetime on the interpretation of nucleation experiments with respect to the first nucleation theorem. *Atmospheric Chemistry and Physics, 13*(22), 11465-11471.

Ehrhart, S., Ickes, L., Almeida, J., Amorim, A., Barmet, P., Bianchi, F., . . . Curtius, J. (2016). Comparison of the SAWNUC model with CLOUD measurements of sulphuric acid-water nucleation. *Journal of Geophysical Research: Atmospheres, 121*(20), 12,401-412,414.

Eisele, F. L., & Hanson, D. R. (2000). First Measurement of Prenucleation Molecular Clusters. *The Journal of Physical Chemistry A, 104*(4), 830-836.

Eisele, F. L., & Tanner, D. J. (1993). Measurement of the gas phase concentration of H_2SO_4 and methane sulfonic acid and estimates of H_2SO_4 production and loss in the atmosphere. *Journal of Geophysical Research: Atmospheres, 98*(D5), 9001-9010.

Elm, J. (2019). An Atmospheric Cluster Database Consisting of Sulfuric Acid, Bases, Organics, and Water. *ACS Omega, 4*(6), 10965-10974.

Elm, J., Jen, C. N., Kurtén, T., & Vehkamäki, H. (2016). Strong Hydrogen Bonded Molecular Interactions between Atmospheric Diamines and Sulfuric Acid. *The Journal of Physical Chemistry A, 120*(20), 3693-3700.

Elm, J., Kubečka, J., Besel, V., Jääskeläinen, M. J., Halonen, R., Kurtén, T., & Vehkamäki, H. (2020). Modeling the formation and growth of atmospheric molecular clusters: A review. *Journal of Aerosol Science, 149*, 105621.

Elm, J., Kurtén, T., Bilde, M., & Mikkelsen, K. V. (2014). Molecular Interaction of Pinic Acid with Sulfuric Acid: Exploring the Thermodynamic Landscape of Cluster Growth. *The Journal of Physical Chemistry A, 118*(36), 7892-7900.

Elm, J., Myllys, N., & Kurtén, T. (2017). What Is Required for Highly Oxidized Molecules To Form Clusters with Sulfuric Acid? *The Journal of Physical Chemistry A, 121*(23), 4578-4587.

Elm, J., Passananti, M., Kurtén, T., & Vehkamäki, H. (2017). Diamines Can Initiate New Particle Formation in the Atmosphere. *The Journal of Physical Chemistry A, 121*(32), 6155-6164.

Fárník, M., & Lengyel, J. (2018). Mass spectrometry of aerosol particle analogues in molecular beam experiments. *Mass Spectrometry Reviews, 37*(5), 630-651.

Feder, J., Russell, K. C., Lothe, J., & Pound, G. M. (1966). Homogeneous nucleation and growth of droplets in vapours. *Advances in Physics, 15*(57), 111-178.

Ferreiro, J. J., Chakrabarty, S., Schläppi, B., & Signorell, R. (2016). Observation of propane cluster size distributions during nucleation and growth in a Laval expansion. *The Journal of Chemical Physics, 145*, 211907-211907.

Fletcher, N. H. (1958). Size Effect in Heterogeneous Nucleation. *The Journal of Chemical Physics, 29*(3), 572-576.

Ford, I. J. (1996). Thermodynamic properties of critical clusters from measurements of vapour–liquid homogeneous nucleation rates. *The Journal of Chemical Physics, 105*(18), 8324-8332.

Ford, I. J. (1997). Nucleation theorems, the statistical mechanics of molecular clusters, and a revision of classical nucleation theory. *Physical Review E, 56*(5), 5615-5629.

Frege, C., Ortega, I. K., Rissanen, M. P., Praplan, A. P., Steiner, G., Heinritzi, M., . . . Baltensperger, U. (2018). Influence of temperature on the molecular composition of ions and charged clusters during pure biogenic nucleation. *Atmos. Chem. Phys., 18*(1), 65-79.

Frenkel, D., & Smit, B. (2002). Understanding molecular simulation : from algorithms to applications. 2nd ed.

Gamero-Castaño, M., & de la Mora, J. F. (2002). Ion-induced nucleation: Measurement of the effect of embryo's size and charge state on the critical supersaturation. *The Journal of Chemical Physics, 117*(7), 3345-3353.

Gelbard, F., & Seinfeld, J. H. (1978). Numerical solution of the dynamic equation for particulate systems. *Journal of Computational Physics, 28*(3), 357-375.

Gelbard, F., & Seinfeld, J. H. (1979). The general dynamic equation for aerosols. Theory and application to aerosol formation and growth. *Journal of Colloid and Interface Science, 68*(2), 363-382.

Gelbard, F., Tambour, Y., & Seinfeld, J. H. (1980). Sectional representations for simulating aerosol dynamics. *Journal of Colloid and Interface Science, 76*(2), 541-556.

Ghosh, D., Bergmann, D., Schwering, R., Wölk, J., Strey, R., Tanimura, S., & Wyslouzil, B. E. (2010). Homogeneous nucleation of a homologous series of n-alkanes ($C_i H_{2i+2}$, i= 7--10) in a supersonic nozzle. *The Journal of Chemical Physics, 132*, 024307-024307.

Gordon, H., Kirkby, J., Baltensperger, U., Bianchi, F., Breitenlechner, M., Curtius, J., . . . Carslaw, K. S. (2017). Causes and importance of new particle formation in the present-day and preindustrial atmospheres. *Journal of Geophysical Research: Atmospheres, 122*(16), 8739-8760.

Goumans, T. P. M., & Bromley, S. T. (2012). Efficient nucleation of stardust silicates via heteromolecular homogeneous condensation. *Monthly Notices of the Royal Astronomical Society, 420*(4), 3344-3349.

Guo, S., Hu, M., Peng, J., Wu, Z., Zamora, M. L., Shang, D., . . . Zhang, R. (2020). Remarkable nucleation and growth of ultrafine particles from vehicular exhaust. *Proceedings of the National Academy of Sciences, 117*(7), 3427.

Guo, S., Hu, M., Zamora, M. L., Peng, J., Shang, D., Zheng, J., . . . Zhang, R. (2014). Elucidating severe urban haze formation in China. *Proceedings of the National Academy of Sciences, 111*(49), 17373.

Haghighi, M., Hawboldt, K. A., & Abedinzadegan Abdi, M. (2015). Supersonic gas separators: Review of latest developments. *Journal of Natural Gas Science and Engineering, 27*, 109-121.

Halonen, R., Zapadinsky, E., Kurtén, T., Vehkamäki, H., & Reischl, B. (2019). Rate enhancement in collisions of sulfuric acid molecules due to long-range intermolecular forces. *Atmos. Chem. Phys., 19*(21), 13355-13366.

Halonen, R., Zapadinsky, E., & Vehkamäki, H. (2018). Deviation from equilibrium conditions in molecular dynamic simulations of homogeneous nucleation. *The Journal of Chemical Physics, 148*(16), 164508.

Hänggi, P., Talkner, P., & Borkovec, M. (1990). Reaction-rate theory: fifty years after Kramers. *Reviews of Modern Physics, 62*(2), 251-341.

Hanson, D. R., & Eisele, F. L. (2002). Measurement of prenucleation molecular clusters in the NH_3, H_2SO_4, H_2O system. *Journal of Geophysical Research: Atmospheres, 107*(D12), AAC 10-11-AAC 10-18.

Hanson, D. R., & Lovejoy, E. R. (2006). Measurement of the Thermodynamics of the Hydrated Dimer and Trimer of Sulfuric Acid. *The Journal of Physical Chemistry A, 110*(31), 9525-9528.

Heinritzi, M., Simon, M., Steiner, G., Wagner, A. C., Kürten, A., Hansel, A., & Curtius, J. (2016). Characterization of the mass-dependent transmission efficiency of a CIMS. *Atmospheric Measurement Techniques, 9*(4), 1449-1460.

Henschel, H., Kurtén, T., & Vehkamäki, H. (2016). Computational Study on the Effect of Hydration on New Particle Formation in the Sulfuric Acid/Ammonia and Sulfuric Acid/Dimethylamine Systems. *The Journal of Physical Chemistry A, 120*(11), 1886-1896.

Henschel, H., Navarro, J. C. A., Yli-Juuti, T., Kupiainen-Määttä, O., Olenius, T., Ortega, I. K., . . . Vehkamäki, H. (2014). Hydration of Atmospherically Relevant Molecular Clusters: Computational Chemistry and Classical Thermodynamics. *The Journal of Physical Chemistry A, 118*(14), 2599-2611.

Horsch, M., Vrabec, J., & Hasse, H. (2008). Modification of the classical nucleation theory based on molecular simulation data for surface tension, critical nucleus size, and nucleation rate. *Physical Review E, 78*(1), 011603.

Hyttinen, N., Kupiainen-Määttä, O., Rissanen, M. P., Muuronen, M., Ehn, M., & Kurtén, T. (2015). Modeling the Charging of Highly Oxidized Cyclohexene Ozonolysis Products Using Nitrate-Based Chemical Ionization. *The Journal of Physical Chemistry A, 119*(24), 6339-6345.

Hyttinen, N., Otkjær, R. V., Iyer, S., Kjaergaard, H. G., Rissanen, M. P., Wennberg, P. O., & Kurtén, T. (2018). Computational Comparison of Different Reagent Ions in the Chemical Ionization of Oxidized Multifunctional Compounds. *The Journal of Physical Chemistry A, 122*(1), 269-279.

Hyttinen, N., Rissanen, M. P., & Kurtén, T. (2017). Computational Comparison of Acetate and Nitrate Chemical Ionization of Highly Oxidized Cyclohexene Ozonolysis Intermediates and Products. *The Journal of Physical Chemistry A, 121*(10), 2172-2179.

Iyer, S., Lopez-Hilfiker, F., Lee, B. H., Thornton, J. A., & Kurtén, T. (2016). Modeling the Detection of Organic and Inorganic Compounds Using Iodide-Based Chemical Ionization. *The Journal of Physical Chemistry A, 120*(4), 576-587.

Jen, C. N., Bachman, R., Zhao, J., McMurry, P. H., & Hanson, D. R. (2016a). Diamine-sulfuric acid reactions are a potent source of new particle formation. *Geophysical Research Letters, 43*(2), 867-873.

Jen, C. N., Hanson, D. R., & McMurry, P. H. (2015). Toward Reconciling Measurements of Atmospherically Relevant Clusters by Chemical Ionization Mass Spectrometry and Mobility Classification/Vapor Condensation. *Aerosol Science and Technology, 49*(1), i-iii.

Jen, C. N., McMurry, P. H., & Hanson, D. R. (2014). Stabilization of sulfuric acid dimers by ammonia, methylamine, dimethylamine, and trimethylamine. *Journal of Geophysical Research: Atmospheres, 119*(12), 7502-7514.

Jen, C. N., Zhao, J., McMurry, P. H., & Hanson, D. R. (2016b). Chemical ionization of clusters formed from sulfuric acid and dimethylamine or diamines. *Atmospheric Chemistry and Physics, 16*(19), 12513-12529.

Jiang, J., Zhao, J., Chen, M., Eisele, F. L., Scheckman, J., Williams, B. J., . . . McMurry, P. H. (2011). First Measurements of Neutral Atmospheric Cluster and 1–2 nm Particle Number Size Distributions During Nucleation Events. *Aerosol Science and Technology, 45*(4), ii-v.

Johnston, M. V., & Kerecman, D. E. (2019). Molecular Characterization of Atmospheric Organic Aerosol by Mass Spectrometry. *Annual Review of Analytical Chemistry, 12*(1), 247-274.

Jokinen, T., Sipilä, M., Junninen, H., Ehn, M., Lönn, G., Hakala, J., . . . Worsnop, D. R. (2012). Atmospheric sulphuric acid and neutral cluster measurements using CI-APi-TOF. *Atmospheric Chemistry and Physics, 12*(9), 4117-4125.

Julin, J., Napari, I., Merikanto, J., & Vehkamäki, H. (2008). Equilibrium sizes and formation energies of small and large Lennard-Jones clusters from molecular dynamics: A consistent comparison to Monte Carlo simulations and density functional theories. *The Journal of Chemical Physics, 129*(23), 234506.

Junninen, H., Ehn, M., Petäjä, T., Luosujärvi, L., Kotiaho, T., Kostiainen, R., . . . Worsnop, D. R. (2010). A high-resolution mass spectrometer to measure atmospheric ion composition. *Atmospheric Measurement Techniques, 3*(4), 1039-1053.

Kalikmanov, V. I. (2013). *Nucleation theory.* (Vol. 860). Netherland, Heidelberg: Springer.

Kammler, H. K., Mädler, L., & Pratsinis, S. E. (2001). Flame Synthesis of Nanoparticles. *Chemical Engineering & Technology, 24*(6), 583-596.

Kangasluoma, J., Cai, R., Jiang, J., Deng, C., Stolzenburg, D., Ahonen, L. R., . . . Lehtipalo, K. (2020). Overview of measurements and current instrumentation for 1–10 nm aerosol particle number size distributions. *Journal of Aerosol Science, 148*, 105584.

Kangasluoma, J., & Kontkanen, J. (2017). On the sources of uncertainty in the sub-3nm particle concentration measurement. *Journal of Aerosol Science, 112*, 34-51.

Kashchiev, D. (1982). On the relation between nucleation work, nucleus size, and nucleation rate. *The Journal of Chemical Physics, 76*, 5098-5102.

Kashchiev, D. (2000). Nucleation : basic theory with applications: Butterworth-Heinemann.

Kathmann, S. M., Schenter, G. K., Garrett, B. C., Chen, B., & Siepmann, J. I. (2009). Thermodynamics and Kinetics of Nanoclusters Controlling Gas-to-Particle Nucleation. *The Journal of Physical Chemistry C, 113*(24), 10354-10370.

Kazil, J., Stier, P., Zhang, K., Quaas, J., Kinne, S., O'Donnell, D., . . . Feichter, J. (2010). Aerosol nucleation and its role for clouds and Earth's radiative forcing in the aerosol-climate model ECHAM5-HAM. *Atmos. Chem. Phys., 10*(22), 10733-10752.

Kerminen, V.-M., Chen, X., Vakkari, V., Petäjä, T., Kulmala, M., & Bianchi, F. (2018). Atmospheric new particle formation and growth: review of field observations. *Environmental Research Letters, 13*(10), 103003.

Khan, A., Heath, C. H., Dieregsweiler, U. M., Wyslouzil, B. E., & Strey, R. (2003). Homogeneous nucleation rates for D_2O in a supersonic Laval nozzle. *The Journal of Chemical Physics, 119*, 3138-3147.

Kildgaard, J. V., Mikkelsen, K. V., Bilde, M., & Elm, J. (2018a). Hydration of Atmospheric Molecular Clusters II: Organic Acid–Water Clusters. *The Journal of Physical Chemistry A, 122*(43), 8549-8556.

Kildgaard, J. V., Mikkelsen, K. V., Bilde, M., & Elm, J. (2018b). Hydration of Atmospheric Molecular Clusters: A New Method for Systematic Configurational Sampling. *The Journal of Physical Chemistry A, 122*(22), 5026-5036.

Kirkby, J., Duplissy, J., Sengupta, K., Frege, C., Gordon, H., Williamson, C., . . . Curtius, J. (2016). Ion-induced nucleation of pure biogenic particles. *Nature, 533*(7604), 521-526.

Kommu, S., Khomami, B., & Biswas, P. (2004a). Simulation of aerosol dynamics and transport in chemically reacting particulate matter laden flows. Part I: Algorithm development and validation. *Chemical Engineering Science, 59*(2), 345-358.

Kommu, S., Khomami, B., & Biswas, P. (2004b). Simulation of aerosol dynamics and transport in chemically reacting particulate matter laden flows. Part II: Application to CVD reactors. *Chemical Engineering Science, 59*(2), 359-371.

Krohn, J., Lippe, M., Li, C., & Signorell, R. (2020). Carbon Dioxide and Propane Nucleation: The Emergence of a Nucleation Barrier. *Physical Chemistry Chemical Physics, 22*(28), 15986-15998.

Kuang, C., McMurry, P. H., & McCormick, A. V. (2009). Determination of cloud condensation nuclei production from measured new particle formation events. *Geophysical Research Letters, 36*(9).

Kuang, C., McMurry, P. H., McCormick, A. V., & Eisele, F. L. (2008). Dependence of nucleation rates on sulfuric acid vapor concentration in diverse atmospheric locations. *Journal of Geophysical Research: Atmospheres, 113*(D10).

Kulmala, M., Petäjä, T., Ehn, M., Thornton, J., Sipilä, M., Worsnop, D. R., & Kerminen, V. M. (2014). Chemistry of Atmospheric Nucleation: On the Recent Advances on Precursor Characterization and Atmospheric Cluster Composition in Connection with Atmospheric New Particle Formation. *Annual Review of Physical Chemistry, 65*(1), 21-37.

Kupiainen-Määttä, O., Olenius, T., Korhonen, H., Malila, J., Dal Maso, M., Lehtinen, K., & Vehkamäki, H. (2014). Critical cluster size cannot in practice be determined by slope analysis in atmospherically relevant applications. *Journal of Aerosol Science, 77*, 127-144.

Kürten, A., Jokinen, T., Simon, M., Sipilä, M., Sarnela, N., Junninen, H., . . . Curtius, J. (2014). Neutral molecular cluster formation of sulfuric acid–dimethylamine observed in real time under atmospheric conditions. *Proceedings of the National Academy of Sciences, 111*(42), 15019.

Kürten, A., Li, C., Bianchi, F., Curtius, J., Dias, A., Donahue, N. M., . . . McMurry, P. H. (2018). New particle formation in the sulfuric acid–dimethylamine–water system: reevaluation of CLOUD chamber measurements and comparison to an aerosol nucleation and growth model. *Atmospheric Chemistry and Physics, 18*(2), 845-863.

Kürten, A., Rondo, L., Ehrhart, S., & Curtius, J. (2012). Calibration of a Chemical Ionization Mass Spectrometer for the Measurement of Gaseous Sulfuric Acid. *The Journal of Physical Chemistry A, 116*(24), 6375-6386.

Kurtén, T., Kuang, C., Gómez, P., McMurry, P. H., Vehkamäki, H., Ortega, I., . . . Kulmala, M. (2010). The role of cluster energy nonaccommodation in atmospheric sulfuric acid nucleation. *The Journal of Chemical Physics, 132*(2), 024304.

Kurtén, T., Noppel, M., Vehkamäki, H., Salonen, M., & Kulmala, M. (2007). Quantum chemical studies of hydrate formation of H_2SO_4 and HSO_4.

Laasonen, K., Wonczak, S., Strey, R., & Laaksonen, A. (2000). Molecular dynamics simulations of gas–liquid nucleation of Lennard-Jones fluid. *The Journal of Chemical Physics, 113*(21), 9741-9747.

Lee, S.-H., Gordon, H., Yu, H., Lehtipalo, K., Haley, R., Li, Y., & Zhang, R. (2019). New Particle Formation in the Atmosphere: From Molecular Clusters to Global Climate. *Journal of Geophysical Research: Atmospheres, 124*(13), 7098-7146.

Lee, S., Hoobler, R. J., & Leone, S. R. (2000). A pulsed Laval nozzle apparatus with laser ionization mass spectroscopy for direct measurements of rate coefficients at low temperatures with condensable gases. *Review of Scientific Instruments, 71*(4), 1816-1823.

Lehtipalo, K., Yan, C., Dada, L., Bianchi, F., Xiao, M., Wagner, R., . . . Worsnop, D. R. (2018). Multicomponent new particle formation from sulfuric acid, ammonia, and biogenic vapors. *Science Advances, 4*(12), eaau5363.

Leiminger, M., Feil, S., Mutschlechner, P., Ylisirniö, A., Gunsch, D., Fischer, L., . . . Steiner, G. (2019). Characterisation of the transfer of cluster ions through an atmospheric pressure interface time-of-flight mass spectrometer with hexapole ion guides. *Atmospheric Measurement Techniques, 12*(10), 5231-5246.

Li, C., Lippe, M., Krohn, J., & Signorell, R. (2019). Extraction of monomer-cluster association rate constants from water nucleation data measured at extreme supersaturations. *The Journal of Chemical Physics, 151*(9), 094305.

Li, C., & McMurry, P. H. (2018). Errors in nanoparticle growth rates inferred from measurements in chemically reacting aerosol systems. *Atmospheric Chemistry and Physics, 18*(12), 8979-8993.

Li, S., Ren, Y., Biswas, P., & Tse, S. D. (2016). Flame aerosol synthesis of nanostructured materials and functional devices: Processing, modeling, and diagnostics. *Progress in Energy and Combustion Science, 55*, 1-59.

Lin, Y., Ji, Y., Li, Y., Secrest, J., Xu, W., Xu, F., . . . Zhang, R. (2019). Interaction between succinic acid and sulfuric acid–base clusters. *Atmos. Chem. Phys., 19*(12), 8003-8019.

Lippe, M., Chakrabarty, S., Ferreiro, J. J., Tanaka, K. K., & Signorell, R. (2018). Water nucleation at extreme supersaturation. *Journal of Chemical Physics, 149*(24), 244303.

Lippe, M., Szczepaniak, U., Hou, G.-L., Chakrabarty, S., Ferreiro, J. J., Chasovskikh, E., & Signorell, R. (2019). Infrared Spectroscopy and Mass Spectrometry of CO_2 Clusters during Nucleation and Growth. *Journal of Physical Chemistry A, 123*(12), 2426-2437.

Litman, J. H., Yoder, B. L., Schläppi, B., & Signorell, R. (2013). Sodium-doping as a reference to study the influence of intracluster chemistry on the fragmentation of weakly-bound clusters upon vacuum ultraviolet photoionization. *Phys. Chem. Chem. Phys., 15*, 940-949.

Liu, L., Zhong, J., Vehkamäki, H., Kurtén, T., Du, L., Zhang, X., . . . Zeng, X. C. (2019). Unexpected quenching effect on new particle formation from the atmospheric reaction of methanol with SO_3. *Proceedings of the National Academy of Sciences, 116*(50), 24966.

Looijmans, K. N. H., Luijten, C. C. M., & van Dongen, M. E. H. (1995). Binary nucleation rate measurements of n‐nonane/methane at high pressures. *The Journal of Chemical Physics, 103*(4), 1714-1717.

Loukonen, V., Bork, N., & Vehkamäki, H. (2014a). From collisions to clusters: first steps of sulphuric acid nanocluster formation dynamics. *Molecular Physics, 112*(15), 1979-1986.

Loukonen, V., Kuo, I. F. W., McGrath, M. J., & Vehkamäki, H. (2014b). On the stability and dynamics of (sulfuric acid)(ammonia) and (sulfuric acid)(dimethylamine) clusters: A first-principles molecular dynamics investigation. *Chemical Physics, 428*, 164-174.

Loukonen, V., Kurtén, T., Ortega, I. K., Vehkamäki, H., Pádua, A. A. H., Sellegri, K., & Kulmala, M. (2010). Enhancing effect of dimethylamine in sulfuric acid nucleation in the presence of water – a computational study. *Atmospheric Chemistry and Physics, 10*(10), 4961-4974.

Lovejoy, E. R., Curtius, J., & Froyd, K. D. (2004). Atmospheric ion-induced nucleation of sulfuric acid and water. *Journal of Geophysical Research: Atmospheres, 109*(D8).

Lümmen, N., & Kraska, T. (2006). Influence of the carrier gas on the formation of iron nano-particles from the gas phase: A molecular dynamics simulation study. *Computational Materials Science, 35*(3), 210-215.

Malila, J., McGraw, R., Laaksonen, A., & Lehtinen, K. E. J. (2015). Communication: Kinetics of scavenging of small, nucleating clusters: First nucleation theorem and sum rules. *The Journal of Chemical Physics, 142*(1), 011102.

Manka, A. A., Brus, D., Hyvärinen, A.-P., Lihavainen, H., Wölk, J., & Strey, R. (2010). Homogeneous water nucleation in a laminar flow diffusion chamber. *The Journal of Chemical Physics, 132*(24), 244505.

Matsubara, H., Koishi, T., Ebisuzaki, T., & Yasuoka, K. (2007). Extended study of molecular dynamics simulation of homogeneous vapor-liquid nucleation of water. *J. Chem. Phys., 127*, 214507-214507.

McGrath, M. J., Olenius, T., Ortega, I. K., Loukonen, V., Paasonen, P., Kurtén, T., . . . Vehkamäki, H. (2012). Atmospheric Cluster Dynamics Code: a flexible method for solution of the birth-death equations. *Atmospheric Chemistry and Physics, 12*(5), 2345-2355.

McGraw, R., & LaViolette, R. A. (1995). Fluctuations, temperature, and detailed balance in classical nucleation theory. *The Journal of Chemical Physics, 102*(22), 8983-8994.

McGraw, R., & Wu, D. T. (2003). Kinetic extensions of the nucleation theorem. *The Journal of Chemical Physics, 118*(20), 9337-9347.

McGraw, R., & Zhang, R. (2008). Multivariate analysis of homogeneous nucleation rate measurements. Nucleation in the p-toluic acid/sulfuric acid/water system. *The Journal of Chemical Physics, 128*(6), 064508.

McKenzie, M. E., & Chen, B. (2006). Unravelling the Peculiar Nucleation Mechanisms for Non-Ideal Binary Mixtures with Atomistic Simulations. *The Journal of Physical Chemistry B, 110*(8), 3511-3516.

McMurry, P. H., & Li, C. (2017). The dynamic behavior of nucleating aerosols in constant reaction rate systems: Dimensional analysis and generic numerical solutions. *Aerosol Science and Technology, 51*(9), 1057-1070.

Merikanto, J., Duplissy, J., Määttänen, A., Henschel, H., Donahue, N. M., Brus, D., . . . Vehkamäki, H. (2016). Effect of ions on sulfuric acid-water binary particle formation: 1. Theory for kinetic- and nucleation-type particle formation and atmospheric implications. *Journal of Geophysical Research: Atmospheres, 121*(4), 1736-1751.

Merikanto, J., Spracklen, D. V., Mann, G. W., Pickering, S. J., & Carslaw, K. S. (2009). Impact of nucleation on global CCN. *Atmospheric Chemistry and Physics, 9*(21), 8601-8616.

Merikanto, J., Vehkamäki, H., & Zapadinsky, E. (2004). Monte Carlo simulations of critical cluster sizes and nucleation rates of water. *The Journal of Chemical Physics, 121*(2), 914-924.

Merikanto, J., Zapadinsky, E., Lauri, A., & Vehkamäki, H. (2007). Origin of the Failure of Classical Nucleation Theory: Incorrect Description of the Smallest Clusters. *Physical Review Letters, 98*(14), 145702.

Mirme, S., & Mirme, A. (2013). The mathematical principles and design of the NAIS – a spectrometer for the measurement of cluster ion and nanometer aerosol size distributions. *Atmos. Meas. Tech., 6*(4), 1061-1071.

Myllys, N., Elm, J., Halonen, R., Kurtén, T., & Vehkamäki, H. (2016). Coupled Cluster Evaluation of the Stability of Atmospheric Acid–Base Clusters with up to 10 Molecules. *The Journal of Physical Chemistry A, 120*(4), 621-630.

Napari, I., Julin, J., & Vehkamäki, H. (2009). Cluster sizes in direct and indirect molecular dynamics simulations of nucleation. *The Journal of Chemical Physics, 131*(24), 244511.

Nellas, R. B., & Chen, B. (2008). Towards understanding the nucleation mechanism for multi-component systems: an atomistic simulation of the ternary nucleation of water/n-nonane/1-butanol. [10.1039/B713189E]. *Physical Chemistry Chemical Physics, 10*(4), 506-514.

Nellas, R. B., Chen, B., & Ilja Siepmann, J. (2007). Dumbbells and onions in ternary nucleation. [10.1039/B705385A]. *Physical Chemistry Chemical Physics, 9*(22), 2779-2781.

Nellas, R. B., Keasler, S. J., Siepmann, J. I., & Chen, B. (2010). Exploring the discrepancies between experiment, theory, and simulation for the homogeneous gas-to-liquid nucleation of 1-pentanol. *The Journal of Chemical Physics, 132*(16), 164517.

Ogunronbi, K. E., Sepehri, A., Chen, B., & Wyslouzil, B. E. (2018). Vapor phase nucleation of the short-chain n-alkanes (n-pentane, n-hexane and n-heptane): Experiments and Monte Carlo simulations. *The Journal of Chemical Physics, 148*(14), 144312.

Ogunronbi, K. E., & Wyslouzil, B. E. (2019). Vapor-phase nucleation of n-pentane, n-hexane, and n-heptane: Critical cluster properties. *The Journal of Chemical Physics, 151*(15), 154307.

Ortega, I. K., Donahue, N. M., Kurtén, T., Kulmala, M., Focsa, C., & Vehkamäki, H. (2016). Can Highly Oxidized Organics Contribute to Atmospheric New Particle Formation? *The Journal of Physical Chemistry A, 120*(9), 1452-1458.

Ortega, I. K., Kupiainen, O., Kurtén, T., Olenius, T., Wilkman, O., McGrath, M. J., . . . Vehkamäki, H. (2012). From quantum chemical formation free energies to evaporation rates. *Atmospheric Chemistry and Physics, 12*(1), 225-235.

Ortega, I. K., Olenius, T., Kupiainen-Määttä, O., Loukonen, V., Kurtén, T., & Vehkamäki, H. (2014). Electrical charging changes the composition of sulfuric acid–ammonia/dimethylamine clusters. *Atmospheric Chemistry and Physics, 14*(15), 7995-8007.

Ouyang, H., Gopalakrishnan, R., & Hogan, C. J. (2012). Nanoparticle collisions in the gas phase in the presence of singular contact potentials. *The Journal of Chemical Physics, 137*(6), 064316.

Oxtoby, D. W., & Kashchiev, D. (1994). A general relation between the nucleation work and the size of the nucleus in multicomponent nucleation. *The Journal of Chemical Physics, 100*(10), 7665-7671.

Passananti, M., Zapadinsky, E., Zanca, T., Kangasluoma, J., Myllys, N., Rissanen, M. P., . . . Vehkamäki, H. (2019). How well can we predict cluster fragmentation inside a mass spectrometer? *Chemical Communications, 55*(42), 5946-5949.

Pathak, H., Wölk, J., Strey, R., & Wyslouzil, B. E. (2014). Co-condensation of nonane and D2O in a supersonic nozzle. *The Journal of Chemical Physics, 140*(3), 034304.

Perraud, V., Xu, J., Gerber, R. B., & Finlayson-Pitts, B. J. (2020). Integrated experimental and theoretical approach to probe the synergistic effect of ammonia in methanesulfonic acid reactions with small alkylamines. *Environmental Science: Processes & Impacts, 22*(2), 305-328.

Rao, N. P., & McMurry, P. H. (1989). Nucleation and Growth of Aerosol in Chemically Reacting Systems: A Theoretical Study of the Near-Collision-Controlled Regime. *Aerosol Science and Technology, 11*(2), 120-132.

Rasmussen, F. R., Kubečka, J., Besel, V., Vehkamäki, H., Mikkelsen, K. V., Bilde, M., & Elm, J. (2020). Hydration of Atmospheric Molecular Clusters III: Procedure for Efficient Free Energy Surface Exploration of Large Hydrated Clusters. *The Journal of Physical Chemistry A*.

Riccobono, F., Schobesberger, S., Scott, C. E., Dommen, J., Ortega, I. K., Rondo, L., . . . Baltensperger, U. (2014). Oxidation Products of Biogenic Emissions Contribute to Nucleation of Atmospheric Particles. *Science, 344*(6185), 717.

Riipinen, I., Pierce, J. R., Yli-Juuti, T., Nieminen, T., Häkkinen, S., Ehn, M., . . . Kulmala, M. (2011). Organic condensation: a vital link connecting aerosol formation to cloud condensation nuclei (CCN) concentrations. *Atmospheric Chemistry and Physics, 11*(8), 3865-3878.

Rissanen, M. P., Mikkilä, J., Iyer, S., & Hakala, J. (2019). Multi-scheme chemical ionization inlet (MION) for fast switching of reagent ion chemistry in atmospheric pressure chemical ionization mass spectrometry (CIMS) applications. *Atmos. Meas. Tech., 12*(12), 6635-6646.

Riva, M., Ehn, M., Li, D., Tomaz, S., Bourgain, F., Perrier, S., & George, C. (2019). CI-Orbitrap: An Analytical Instrument To Study Atmospheric Reactive Organic Species. *Analytical Chemistry, 91*(15), 9419-9423.

Römer, F., & Kraska, T. (2007). Homogeneous nucleation and growth in supersaturated zinc vapor investigated by molecular dynamics simulation. *The Journal of Chemical Physics, 127*(23), 234509.

Rosser, S., & de la Mora, J. F. (2005). Vienna-Type DMA of High Resolution and High Flow Rate. *Aerosol Science and Technology, 39*(12), 1191-1200.

Rowe, B. R., Marquette, J.-B., & Rebrion, C. (1989). Mass-selected ion–molecule reactions at very low temperatures. The CRESUS apparatus. [10.1039/F29898501631]. *Journal of the Chemical Society, Faraday Transactions 2: Molecular and Chemical Physics, 85*(10), 1631-1641.

Saad, M. A. (1985). Compressible fluid flow. *Englewood Cliffs, NJ, Prentice-Hall, Inc., 1985. 570 p.*

Sabbah, H., Biennier, L., Klippenstein, S. J., Sims, I. R., & Rowe, B. R. (2010). Exploring the role of PAHs in the formation of soot: Pyrene dimerization. *The Journal of Physical Chemistry Letters, 1*(19), 2962-2967.

Salvalaglio, M., Tiwary, P., Maggioni, G. M., Mazzotti, M., & Parrinello, M. (2016). Overcoming time scale and finite size limitations to compute nucleation rates from small scale well tempered metadynamics simulations. *The Journal of Chemical Physics, 145*(21), 211925.

Sceats, M. G. (1989). Brownian coagulation in aerosols—the role of long range forces. *Journal of Colloid and Interface Science, 129*(1), 105-112.

Schläppi, B., Litman, J. H., Ferreiro, J. J., Stapfer, D., & Signorell, R. (2015). A pulsed uniform Laval expansion coupled with single photon ionization and mass spectrometric detection for the study of large molecular aggregates. *Physical Chemistry Chemical Physics, 17*(39), 25761-25771.

Seinfeld, J. H., & Pandis, S. N. (2016). *Atmospheric chemistry and physics: from air pollution to climate change* (3rd ed.): John Wiley & Sons.

Senftle, T. P., Hong, S., Islam, M. M., Kylasa, S. B., Zheng, Y., Shin, Y. K., . . . van Duin, A. C. T. (2016). The ReaxFF reactive force-field: development, applications and future directions. *npj Computational Materials, 2*(1), 15011.

Sinha, S., Bhabhe, A., Laksmono, H., Wölk, J., Strey, R., & Wyslouzil, B. (2010). Argon nucleation in a cryogenic supersonic nozzle. *The Journal of Chemical Physics, 132*, 064304-064304.

Sipilä, M., Sarnela, N., Jokinen, T., Henschel, H., Junninen, H., Kontkanen, J., . . . O'Dowd, C. (2016). Molecular-scale evidence of aerosol particle formation via sequential addition of HIO_3. *Nature, 537*(7621), 532-534.

Sipilä, M., Sarnela, N., Jokinen, T., Junninen, H., Hakala, J., Rissanen, M. P., . . . Worsnop, D. R. (2015). Bisulfate – cluster based atmospheric pressure chemical ionization mass spectrometer for high-sensitivity (< 100 ppqV) detection of atmospheric dimethyl amine: proof-of-concept and first ambient data from boreal forest. *Atmospheric Measurement Techniques, 8*(10), 4001-4011.

Spracklen, D. V., Carslaw, K. S., Kulmala, M., Kerminen, V.-M., Sihto, S.-L., Riipinen, I., . . . Lihavainen, H. (2008). Contribution of particle formation to global cloud condensation nuclei concentrations. *Geophysical Research Letters, 35*(6).

Stolzenburg, D., Fischer, L., Vogel, A. L., Heinritzi, M., Schervish, M., Simon, M., . . . Winkler, P. M. (2018). Rapid growth of organic aerosol nanoparticles over a wide tropospheric temperature range. *Proceedings of the National Academy of Sciences, 115*(37), 9122.

Stolzenburg, D., Simon, M., Ranjithkumar, A., Kürten, A., Lehtipalo, K., Gordon, H., . . . Winkler, P. M. (2020). Enhanced growth rate of atmospheric particles from sulfuric acid. *Atmos. Chem. Phys., 20*(12), 7359-7372.

Tanaka, K. K., Kawano, A., & Tanaka, H. (2014). Molecular dynamics simulations of the nucleation of water: Determining the sticking probability and formation energy of a cluster. *The Journal of Chemical Physics, 140*, 114302-114302.

Tanaka, K. K., Tanaka, H., Yamamoto, T., & Kawamura, K. (2011). Molecular dynamics simulations of nucleation from vapor to solid composed of Lennard-Jones molecules. *The Journal of Chemical Physics, 134*(20), 204313-204313.

Tanimura, S., Dieregsweiler, U. M., & Wyslouzil, B. E. (2010). Binary nucleation rates for ethanol/water mixtures in supersonic Laval nozzles. *The Journal of Chemical Physics, 133*(17), 174305.

Tanimura, S., Pathak, H., & Wyslouzil, B. E. (2013). Binary nucleation rates for ethanol/water mixtures in supersonic Laval nozzles: Analyses by the first and second nucleation theorems. *The Journal of Chemical Physics, 139*(17), 174311.

Tanimura, S., Wyslouzil, B. E., & Wilemski, G. (2010). CH_3CH_2OD/D_2O binary condensation in a supersonic Laval nozzle: Presence of small clusters inferred from a macroscopic energy balance. *The Journal of Chemical Physics, 132*(14), 144301.

Tauber, C., Chen, X., Wagner, P. E., Winkler, P. M., Hogan Jr, C. J., & Maißer, A. (2018). Heterogeneous Nucleation onto Monoatomic Ions: Support for the Kelvin-Thomson Theory. *ChemPhysChem, 19*(22), 3144-3149.

Temelso, B., Morrell, T. E., Shields, R. M., Allodi, M. A., Wood, E. K., Kirschner, K. N., . . . Shields, G. C. (2012). Quantum Mechanical Study of Sulfuric Acid Hydration: Atmospheric Implications. *The Journal of Physical Chemistry A, 116*(9), 2209-2224.

ten Wolde, P. R., & Frenkel, D. (1998). Computer simulation study of gas–liquid nucleation in a Lennard-Jones system. *The Journal of Chemical Physics, 109*(22), 9901-9918.

Thomas, J. M., He, S., Larriba-Andaluz, C., DePalma, J. W., Johnston, M. V., & Hogan Jr, C. J. (2016). Ion mobility spectrometry-mass spectrometry examination of the structures, stabilities, and extents

of hydration of dimethylamine–sulfuric acid clusters. *Physical Chemistry Chemical Physics, 18*(33), 22962-22972.

Tröstl, J., Chuang, W. K., Gordon, H., Heinritzi, M., Yan, C., Molteni, U., . . . Baltensperger, U. (2016). The role of low-volatility organic compounds in initial particle growth in the atmosphere. *Nature, 533*, 527.

Tsai, S.-T., Smith, Z., & Tiwary, P. (2019). Reaction coordinates and rate constants for liquid droplet nucleation: Quantifying the interplay between driving force and memory. *The Journal of Chemical Physics, 151*(15), 154106.

Vehkamäki, H. (2006). *Classical nucleation theory in multicomponent systems*: Springer Science & Business Media.

Vehkamäki, H., & Ford, I. J. (2000). Analysis of water–ethanol nucleation rate data with two component nucleation theorems. *The Journal of Chemical Physics, 113*(8), 3261-3269.

Vehkamäki, H., Määttänen, A., Lauri, A., Kulmala, M., Winkler, P., Vrtala, A., & Wagner, P. E. (2007). Heterogeneous multicomponent nucleation theorems for the analysis of nanoclusters. *The Journal of Chemical Physics, 126*(17), 174707.

Vehkamäki, H., McGrath, M. J., Kurtén, T., Julin, J., Lehtinen, K. E. J., & Kulmala, M. (2012). Rethinking the application of the first nucleation theorem to particle formation. *The Journal of Chemical Physics, 136*(9), 094107.

Vehkamäki, H., & Riipinen, I. (2012). Thermodynamics and kinetics of atmospheric aerosol particle formation and growth. *Chemical Society Reviews, 41*(15), 5160-5173.

Viisanen, Y., & Strey, R. (1994). Homogeneous nucleation rates for n-butanol. *The Journal of Chemical Physics, 101*, 7835-7843.

Wang, Z., Wu, Z., Yue, D., Shang, D., Guo, S., Sun, J., . . . Hu, M. (2017). New particle formation in China: Current knowledge and further directions. *Science of The Total Environment, 577*, 258-266.

Wedekind, J., Hyvärinen, A.-P., Brus, D., & Reguera, D. (2008). Unraveling the ``Pressure Effect'' in Nucleation. *Physical Review Letters, 101*(12), 125703.

Wedekind, J., Reguera, D., & Strey, R. (2007). Influence of thermostats and carrier gas on simulations of nucleation. *The Journal of Chemical Physics, 127*(6), 064501.

Wegener, P. P. (1975). Nonequilibrium flow with condensation. *Acta Mechanica, 21*(1), 65-91.

Wegener, P. P., & Wu, B. J. C. (1976). Homogeneous and binary nucleation: new experimental results and comparison with theory. *Faraday Discussions of the Chemical Society, 61*(0), 77-82.

Westervelt, D. M., Pierce, J. R., & Adams, P. J. (2014). Analysis of feedbacks between nucleation rate, survival probability and cloud condensation nuclei formation. *Atmospheric Chemistry and Physics, 14*(11), 5577-5597.

Wilson, C. T. R. (1897). Condensation of water vapour in the presence of dust-free air and other gases. *Philosophical Transactions of the Royal Society A, 189*, 265-307.

Winkler, P. M., Steiner, G., Vrtala, A., Vehkamäki, H., Noppel, M., Lehtinen, K. E. J., . . . Kulmala, M. (2008). Heterogeneous Nucleation Experiments Bridging the Scale from Molecular Ion Clusters to Nanoparticles. *Science, 319*(5868), 1374.

Winkler, P. M., Vrtala, A., Steiner, G., Wimmer, D., Vehkamäki, H., Lehtinen, K. E. J., . . . Wagner, P. E. (2012). Quantitative Characterization of Critical Nanoclusters Nucleated on Large Single Molecules. *Physical Review Letters, 108*(8), 085701.

Wu, J. J., & Flagan, R. C. (1988). A discrete-sectional solution to the aerosol dynamic equation. *Journal of Colloid and Interface Science, 123*(2), 339-352.

Wyslouzil, B. E., & Seinfeld, J. H. (1992). Nonisothermal homogeneous nucleation. *The Journal of Chemical Physics, 97*(4), 2661-2670.

Wyslouzil, B. E., & Wilemski, G. (1995). Binary nucleation kinetics. II. Numerical solution of the birth–death equations. *The Journal of Chemical Physics, 103*(3), 1137-1151.

Wyslouzil, B. E., Wilemski, G., Strey, R., Seifert, S., & Winans, R. E. (2007). Small angle X-ray scattering measurements probe water nanodroplet evolution under highly non-equilibrium conditions. *Physical Chemistry Chemical Physics, 9*, 5353-5358.

Wyslouzil, B. E., & Wölk, J. (2016). Overview: Homogeneous nucleation from the vapor phase—The experimental science. *The Journal of Chemical Physics, 145*(21), 211702.

Xu, W., & Zhang, R. (2012). Theoretical Investigation of Interaction of Dicarboxylic Acids with Common Aerosol Nucleation Precursors. *The Journal of Physical Chemistry A, 116*(18), 4539-4550.

Yang, H., Drossinos, Y., & Hogan, C. J. (2019). Excess thermal energy and latent heat in nanocluster collisional growth. *The Journal of Chemical Physics, 151*(22), 224304.

Yang, H., Goudeli, E., & Hogan, C. J. (2018). Condensation and dissociation rates for gas phase metal clusters from molecular dynamics trajectory calculations. *The Journal of Chemical Physics, 148*(16), 164304.

Yao, L., Garmash, O., Bianchi, F., Zheng, J., Yan, C., Kontkanen, J., . . . Wang, L. (2018). Atmospheric new particle formation from sulfuric acid and amines in a Chinese megacity. *Science, 361*(6399), 278.

Yasuoka, K., & Matsumoto, M. (1998a). Molecular dynamics of homogeneous nucleation in the vapor phase. I. Lennard-Jones fluid. *The Journal of Chemical Physics, 109*(19), 8451-8462.

Yasuoka, K., & Matsumoto, M. (1998b). Molecular dynamics of homogeneous nucleation in the vapor phase. II. Water. *The Journal of Chemical Physics, 109*, 8463-8470.

Yasuoka, K., & Zeng, X. C. (2007). Molecular dynamics of homogeneous nucleation in the vapor phase of Lennard-Jones. III. Effect of carrier gas pressure. *The Journal of Chemical Physics, 126*(12), 124320.

Yu, F. (2006). From molecular clusters to nanoparticles: second-generation ion-mediated nucleation model. *Atmospheric Chemistry and Physics, 6*(12), 5193-5211.

Yu, F., Nadykto, A. B., Herb, J., Luo, G., Nazarenko, K. M., & Uvarova, L. A. (2018). H_2SO_4–H_2O–NH_3 ternary ion-mediated nucleation (TIMN): kinetic-based model and comparison with CLOUD measurements. *Atmospheric Chemistry and Physics, 18*(23), 17451-17474.

Yu, H., Dai, L., Zhao, Y., Kanawade, V. P., Tripathi, S. N., Ge, X., . . . Lee, S.-H. (2017). Laboratory observations of temperature and humidity dependencies of nucleation and growth rates of sub-3 nm particles. *Journal of Geophysical Research: Atmospheres, 122*(3), 1919-1929.

Yu, H., McGraw, R., & Lee, S.-H. (2012). Effects of amines on formation of sub-3 nm particles and their subsequent growth. *Geophysical Research Letters, 39*(2).

Zanca, T., Kubečka, J., Zapadinsky, E., Passananti, M., Kurtén, T., & Vehkamäki, H. (2020). Highly oxygenated organic molecule cluster decomposition in atmospheric pressure interface time-of-flight mass spectrometers. *Atmospheric Measurement Techniques, 13*(7), 3581-3593.

Zapadinsky, E., Passananti, M., Myllys, N., Kurtén, T., & Vehkamäki, H. (2019). Modeling on Fragmentation of Clusters inside a Mass Spectrometer. *The Journal of Physical Chemistry A, 123*(2), 611-624.

Zeldovich, J. B. (1943). On the theory of new phase formation: cavitation. *Acta Physicochem., USSR, 18*(1), 1-22.

Zhang, R., Khalizov, A., Wang, L., Hu, M., & Xu, W. (2012). Nucleation and Growth of Nanoparticles in the Atmosphere. *Chemical Reviews, 112*(3), 1957-2011.

Zhang, R., Suh, I., Zhao, J., Zhang, D., Fortner, E. C., Tie, X., . . . Molina, M. J. (2004). Atmospheric New Particle Formation Enhanced by Organic Acids. *Science, 304*(5676), 1487.

Zhao, J., Eisele, F. L., Titcombe, M., Kuang, C., & McMurry, P. H. (2010). Chemical ionization mass spectrometric measurements of atmospheric neutral clusters using the cluster-CIMS. *Journal of Geophysical Research: Atmospheres, 115*(D8).

Zhao, J., Khalizov, A., Zhang, R., & McGraw, R. (2009). Hydrogen-Bonding Interaction in Molecular Complexes and Clusters of Aerosol Nucleation Precursors. *The Journal of Physical Chemistry A, 113*(4), 680-689.

Zhao, J., Smith, J. N., Eisele, F. L., Chen, M., Kuang, C., & McMurry, P. H. (2011). Observation of neutral sulfuric acid-amine containing clusters in laboratory and ambient measurements. *Atmospheric Chemistry and Physics, 11*(21), 10823-10836.

Zhao, R. (2018). The Recent Development and Application of Chemical Ionization Mass Spectrometry in Atmospheric Chemistry *Encyclopedia of Analytical Chemistry* (pp. 1-33).

Zhukhovitskii, D. I. (2016). Enhancement of the droplet nucleation in a dense supersaturated Lennard-Jones vapor. *The Journal of Chemical Physics, 144*(18), 184701.

Zipoli, F., Laino, T., Stolz, S., Martin, E., Winkelmann, C., & Curioni, A. (2013). Improved coarse-grained model for molecular-dynamics simulations of water nucleation. *The Journal of Chemical Physics, 139*, 094501-094501.

Zollner, J. H., Glasoe, W. A., Panta, B., Carlson, K. K., McMurry, P. H., & Hanson, D. R. (2012). Sulfuric acid nucleation: power dependencies, variation with relative humidity, and effect of bases. *Atmospheric Chemistry and Physics, 12*(10), 4399-4411.

Chenxi Li received a BEng in Engineering Physics at Tsinghua university. He obtained his PhD at the University of Minnesota in mechanical engineering. His research interest mainly lies in gas phase nucleation and particle growth, aerosol system dynamics, and analytical techniques including ion-mobility-mass spectrometry. Presently, he is an assistant professor in the department of Environmental Science and Engineering in Shanghai Jiao Tong University.


Copyright UHHCUI, Peter Garten

Ruth Signorell received her MSc and PhD degrees in the field of molecular spectroscopy from the Swiss Federal Institute of Technology (ETH). She started her aerosol research in 2002 as an Assistant Professor at the Georg-August University Goettingen, Germany. Between 2005 and 2012, she was first Associate Professor and later Full Professor at the University of British Columbia in Vancouver, Canada. In 2012, she returned to Switzerland to take up a position as a Full Professor for Physical Chemistry in the Department of Chemistry and Applied Biosciences at ETH Zuerich. Her research interests focus on spectroscopic studies of fundamental processes in aerosol particles and molecular clusters.